RULE BASED APPROACH FOR CLASSIFYING CROP PARCELS USING MULTI-SENSOR AND MULTI-TEMPORAL IMAGES

EMANI RAJA RAGHUDEEP
March, 2014

SUPERVISORS:
Ms. Dr. ir. Wietske Bijker
Mr. Dr. V.A. Tolpekin

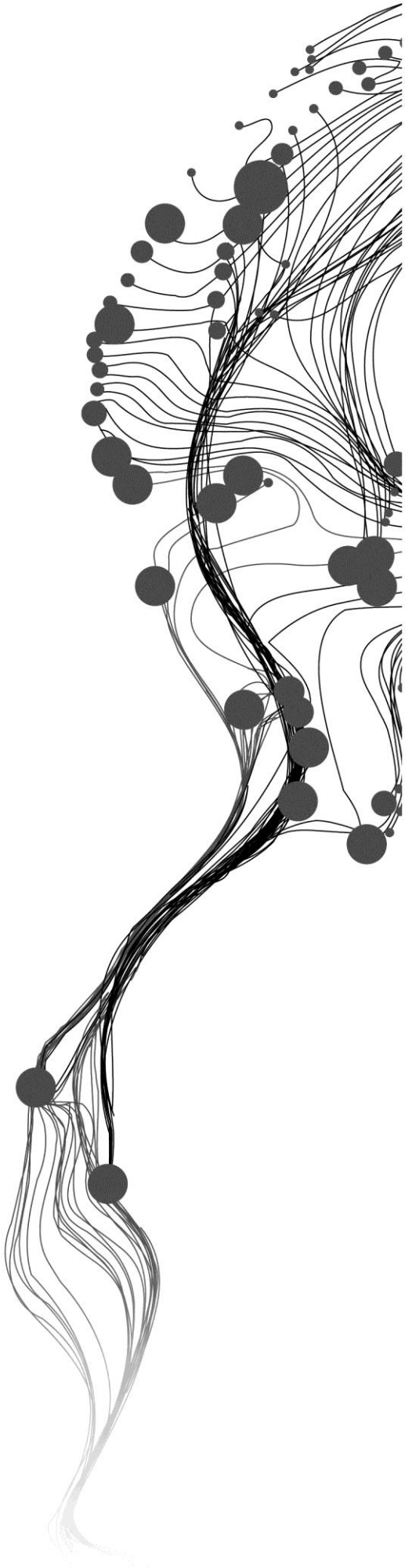

RULE BASED APPROACH FOR CLASSIFYING CROP PARCELS USING MULTI-SENSOR AND MULTI-TEMPORAL IMAGES

EMANI RAJA RAGHUDEEP
Enschede, the Netherlands, March, 2014

Thesis submitted to the Faculty of Geo-Information Science and Earth Observation of the University of Twente in partial fulfilment of the requirements for the degree of Master of Science in Geo-information Science and Earth Observation.
Specialization: Geoinformatics

SUPERVISORS:
Ms Dr.Ir. W. Bijker
Dr. V.A. Tolpekin

THESIS ASSESSMENT BOARD:
Prof.Dr.Ir. A. Stein (Chair)
Ir. C.J. van der Sande (External Examiner, NEO For earth observation)

ABSTRACT

Demand of agricultural map is getting very prominent these days. It is being used in many government organisations for the allocation of subsidy and in the municipal organisation for keeping all the records regarding crop fields. Rise of multi-sensor satellite data is an answer to create maps at a faster pace which would be used by different organisations. Multi-sensor data is having different spatial, spectral and radiometric resolutions, handling such data needs some pre-processing of the images. In the present research one of the images is geometrically transformed and all the images are then radiometrically calibrated using linear contrast stretch method by which 16 bit data is converted to 8 bit where the 8 bit data is linearly stretched. Using object oriented approach, parcel statistics have been extracted which comprised of mean and standard deviation of all the bands of a pixel in a parcel. Using the reference data, parcel types were plotted in feature space of near infra-red and red bands. Based on the feature space, rules were formed using normalized differential vegetation index and standard deviation for three images and ratio vegetation index was used for one of the image. Classes such as uniform normal vegetation, non-uniform normal vegetation, sparse vegetation, bare land, dense vegetation and mixed parcels were formed for all the images. Based on these classes, a final classification was applied using the majority characteristic rule by using half the reference data for training and the rest of validation of a particular parcel type.

Final accuracy was calculated using confusion matrix, where an accuracy of 38% was obtained. Mixed parcels were not taken into account for the classification of different parcel types but rather they were made a separate class which is one of the reasons for low accuracy.

Keywords: multi-sensor images, radiometric calibration, object oriented approach, rule based approach

ACKNOWLEDGEMENTS

All thanks to Almighty God for successful completion of this thesis.

I express appreciation to my supervisors Ms. Dr. Ir. Wietske Bijker and Dr. Valentyn Tolpekin for their continuous encouragement, guidance and suggestions throughout the research period.

For the opportunity given to me to study at ITC I greatly appreciate Punjab National bank for giving me the study loan and my parents for support they always showed.

I am also very grateful to Ir. C.J. van der Sande of NEO For earth observation for his contributions and particularly for providing me data.

I appreciate the contribution of my friends; Abhishek, Akshay, Gunamani, Jyothi, Goke, Shahriar Rahman, Akhil and my dearest parents for their invaluable contributions and encouragement.

Finally, I appreciate my sister Harshi for her encouragement and prayers.

TABLE OF CONTENTS

LIST OF FIGURES

LIST OF TABLES

1. INTRODUCTION

Food is any substance when consumed gives energy to the body, which in other sense can be termed as saviour of life. Digging into the history of obtaining food, it is classified into two methods, one by "Hunting & gathering" and the other through "Agriculture". The later part of obtaining food i.e. through Agriculture has gained a lot of prominence in the history of mankind. Right from the Neolithic age to the present Information age, practice of cultivation has seen a drastic change. Use of fertilizers, pesticides and mechanization of farming tools has tremendously increased the production of food all over the world. This made agriculture an important subject of study in the world economy.

1.1. Agriculture and Climate in Netherlands

Broadly, agriculture can be divided into two parts which are; the cultivation through crops and animal husbandry. Crop cultivation is always seen as an instrument in shaping the human civilization throughout the time. There are a variety of crops grown in Netherlands; some of the most important are potatoes, wheat, barley, maize, sugar beet etc. Based on the 2011 statistics from Food and Agriculture Organisation of United Nations (FAO), it has 1894.8 (1000 Ha) of agricultural area and products such as winter wheat, potatoes, sugar-beet are one of the highest per-hectare yield in the world (FAO, 2012).

Climate in Netherlands is temperate maritime climate with cooler summers and milder winters. Research in the recent decade has shown that the long term changes in mean temperature or precipitation with other conventional pressures would have a significant role in agricultural productivity (Kurukulasuriya & Rosenthal, 2003).

1.1.1. Understanding Common Agricultural Policy (CAP)

The Common Agricultural Policy of the European Union was established in 1962 with its main emphasis always to ensure better living conditions for the farmers and to supply safe food at cheaper rates to the people according to the European Commission . There are several policy areas in CAP, where the area of Direct Support is useful for this study.

Direct support policy area is divided into three types as direct payments, Cross-compliance and Integrated Administration & Control system (IACS) where direct payments are single payment schemes to the farmers, cross-compliance is an area where if a farmer does not comply with certain requirements like animal and plant health, environment and animal welfare are subjected to reduction or exclusion from the direct support scheme and finally the IACS under which member states have to take necessary steps to

assure that the transactions financed by European Agricultural Guarantee are carried and executed properly according to European Commission .

1.2. Motivation

As the urbanization got more prominent with the start of industrial age, agriculture started losing its popularity as more people started moving towards the urban centres. With this alarming rate of urbanization, various organizations proposed to introduce subsidies to protect farmer's interest in agriculture. . Thus the birth of Common agricultural policy (CAP) in 1962 by European Union increased the productivity of individual farms and sum total in agricultural production (Reichert, 2006).With the passage of time there has been exploitation of subsidies by farmers funded by the CAP. Some of the control conditions of agricultural subsidies like permanent grasslands, breaking and mowing of grasslands, incorrect crop applications, ineligible features (e.g.: horse boxes etc.) needed to be controlled for the rightful subsidy allocation to farmers. Such violations of subsidy norms by farmers gave rise to the need of classifying crop parcels from time to time and partially automate the control conditions of agricultural subsidy.

1.2.1. Remote sensing in Agricultural Science

It is not new in Agricultural science that remote sensing has been used for crop identification using time series analysis. An extensive research has been done in crop classification like mapping crop patterns using time series analysis of LANDSAT-TM images (Martínez-Casasnovas et al., 2005) which showed the change in crops from year to year. Other interesting research in this field is the identification of crops using harmonic analysis of AVHRR NDVI data (Jakubauskas et al., 2002) which states the differentiation in crops can be found from the change in temporal NDVI values. Presently, Dynamic Time Wrapping has gained a presumable importance in this field because it can exploit temporal distortions and errors (Petitjean et al., 2012). This concept is motivating in dealing with satellite image time series (SITS) as it deals with temporal nature of whole data set without skipping any values (Petitjean et al., 2012).

1.2.2. Rise of multi-sensor satellite data

As of March 2012, a lot of satellite data is available from remote sensing projects like Geo-Eye, World-view, DMC and Pleiades. All these data are of high spatial and radiometric resolution. Using these high resolution images would be advantageous in the present scenario where classified maps of different areas of a particular year are of high demand. The challenge here is taking into account any subset of high resolution images for a season and then using them for crop classification by applying time series analysis methods. One of the problems in using high resolution images is mixed pixels, which makes it difficult to determine the boundary of crop parcels. Using multi-sensor images also focuses on many problems out of which the subtle spectral differences between objects on the ground will be observed differently by multiple sensors, so this can have an impact in classification using multiple sensors.

1.2.3. Problem statement

Based on the context presented above, the research problem can be formulated as to use images from different sources having different spatial, radiometric and spectral resolutions. Later to classify crop parcels using object-based rule-based classification having multiple rule-bases and a polygon layer to provide an object oriented approach. The use of multiple rule-bases can be interesting as each rule base will focus on one sensor and that results can be updated as new sources of data is included in the classification (Richards, 2013a).

1.3. Research Objectives and Questions

1.3.1. Overall Research Objective

To classify different crop types and grassland using multi-sensor and multi-temporal images in an object-based rule-based system.

1.3.2. Specific Objectives

1. To pre-process multi-sensor images through radiometric calibration.
2. To get per parcel statistical information of each image by overlaying vector polygon data.
3. To generate feature spaces of crop parcels and study them by comparing different crop types.
4. To form rules for each sensor image based on the analysis of feature spaces of different crops and the temporal change in crop parcels.
5. To check the accuracy of the classified map using ground truth data.

1.3.3. Research Questions

1. How to handle differences in radiometric resolution in multi sensor images?
2. Does the combined use of multi-sensor images can provide better results in crop identification than single sensor images?
3. How to define rules using feature space of parcels of different crop types and grassland?
4. Is the use of multiple-rule base approach better than single rule base in the present study of crop classification?
5. What would be the performance quality of this classification method in terms of speed and accuracy?

1.4. Innovation

The innovation aimed in this research is the use of multi sensor images, having different spatial, radiometric and spectral resolutions and try to find a method without much changing their unique properties but rather using those for classifying different crop types.

1.5. Thesis Structure

The thesis consists of seven chapters starting from Chapter 1 where an overview of agriculture, climate and Common agriculture policy are stated following which motivation, research objectives and questions are mentioned. Chapter 2 provides literature review on previous studies covering the area of remote

sensing and agriculture, Multi-temporal analysis and finally Multi-sensor analysis. Chapter 3 presents the description of study area with different datasets. Chapter 4 deals with the general methodology adopted to answer the research questions and results are provided in Chapter 5. Discussions and limitation of the research are provided in Chapter 6 and finally the conclusions and recommendations in Chapter 7.

2. LITERATURE REVIEW

The following section will discuss the previous research that has been carried out in the present field of study.

2.1. Concept of digital number (DN) and surface reflectance

A digital number (DN) at each pixel is defined as the integrated radiance converted to an electrical signal and quantified as an integer value (Schowengerdt, 2007). According to Moran et al. (1995), retrieving the surface reflectance from the satellite digital number requires the knowledge of atmospheric conditions and sensor calibration data. The digital numbers (DN) recorded in raw images are not an accurate measure of change over time as they are not only the function of surface conditions but also the periodically variable atmospheric conditions, seasonally variable Earth-Sun distance, solar zenith angle and the sensor calibration (Moran et al., 2001). To achieve at-satellite reflectance which normalizes for variations due to Earth-Sun distance and solar zenith angle, first the raw DN is converted to at-satellite radiance by utilizing gain and offset coefficients for sensor calibration and then the obtained radiances are converted to at-satellite reflectance (Clark et al., 2011). There are various methods which accounts for influencing illumination and atmosphere on-sensor recorded radiance, some of those are normalization to a spectrally flat target or an image average, empirical relationships between radiance and reflectance and radiative transfer models to stimulate the interaction of radiation with atmosphere & surface (Smith & Milton, 1999). Radiative transfer models produces better results compared to other methods but they require measurements of atmospheric variables at the time of acquisition which is difficult to obtain whereas empirical relationships produce acceptable results but only they require measurements of ground reflectance at number of targets (Smith & Milton, 1999). Kowalik et al. (1982) proposed a relation between Landsat digital numbers, surface reflectance and cosine of the solar zenith angle where the relation was used for estimating the ground reflectance of unknown sites from the reflectance of known sites by observing the rate of change of radiance as a function of cosine of solar zenith angle. Masek et al. (2006) used the MODIS adaptive processing system (MODAPS) software architecture developed at NASA Goddard Space Flight Center (GSFC) under the Landsat Ecosystem Disturbance Adaptive Processing System (LEDAPS) for obtaining a Landsat surface reflectance dataset for North America where the digital numbers are first ingested using Hierarchical Data Format-Earth Observing System (HDF-EOS) file formats, calibrated at sensor radiance and finally they are atmospherically converted to surface reflectance using 6S radiative transfer model.

2.2. Phenophase analysis of crop

Crops are grown in well irrigated agricultural fields specially designated for them under specific favorable conditions. They exhibit different features as they grow during their life. The major stages of crop

development are: vegetative, reproduction and maturation. In these stages, growth from seeds into short stems and later into a fully developed plant, flowering of the plant and finally senescence (Meier, 1997). For each stage of phenology a numerical code is assigned and a continuous scale is defined for the whole cycle (Meier, 1997).

	Principal growth stages	
	Stage	Description
Vegetative 00-49	0	Germination / sprouting / bud development
	1	Leaf development (main shoot)
	2	Formation of side shoots / tillering
	3	Stem elongation or rosette growth / shoot development (main shoot)
	4	Development of harvestable vegetative plant parts or vegetatively propagated organs / booting (main shoot)
Reproductive 50-69	5	Inflorescence emergence (main shoot) / heading
	6	Flowering (main shoot)
Maturation 70-99	7	Development of fruit
	8	Ripening or maturity of fruit and seed
	9	Senescence, beginning of dormancy

Figure 2-1: Principal growth stage. First digits (tens) represent principal stages and second digits (units) represent secondary stages of plant development. Source Meier (1997).

2.3. Multi-temporal analysis

Multi-temporal analysis on crops has always been an interesting area of study because of its capability to show change in crop growth and area in different dates, such information can be vital in crop classification. Panigrahy and Sharma (1997) used Red and NIR bands of LISS-1 multi-date data acquired in different crop seasons, this resulted in more than 95% accuracy for the pixels used in validation, similarly they used principal components of multi-date data and to their findings they got similar accuracy, including the transitional phase crop mapping data improved their classification. A hierarchical classification approach for per-plot crop identification was proposed by Foerster et al. (2012), where the classification is based on spectral temporal profile, the method is based on the fact that every crop has its own seasonal spectral behavior over the time and weather may accelerate or delay crop development. Results showed that its accuracy was 7.1% less than Maximum Likelihood Classification but this can be justified by its independence of ground truth information (Foerster et al., 2012). Temporal un-mixing by using independent component analysis for spatial distribution of crop types is an interesting approach, as the individual crops are observed as the mixtures of temporal profiles with a moderate resolution sensor (MODIS) where cultivated fields are smaller than the spatial resolution of the sensor, the major task of

Independent Component Analysis is to decompose these mixed observations into individual crop signals (Ozdogan, 2010). Rule based classification using e-cognition to classify agricultural land using multi temporal images presents a viable approach in object oriented analysis where the vegetation types are discriminated based on inferred differences in phenology, structure, wetness and productivity (Lucas et al., 2007). Xia Zhang et al. (2008) proposed an approach for land cover classification of the North China Plain using MODIS_EVI time series from 2003, in that first they removed the noise and cloud cover using Harmonic Analysis of Time Series (HANTS) and then classified into 100 clusters using ISODATA. To distinguish ambiguous classes they built a decision tree based on five phenology features derived from EVI profiles, Land surface temperature and topographic slope which gave them a promising 75.5% accuracy (Xia Zhang et al., 2008). Van Niel and McVicar (2004) stated that determining the best time of image acquisition for crop discrimination could impact accuracy as much as the classification algorithm and selection of training data. They performed multi-date classification by combining various numbers of bands of Landsat Thematic Mapper data per date into single image stack prior to classification and then extracting maximum accuracy single crop classes from different dates (Van Niel & McVicar, 2004).

2.4. Multi-sensor data analysis

Multi sensor data are valuable for increasing classification accuracies by contributing more information, for example VNIR in optical sensor would contribute information related to chlorophyll content and canopy structure and whereas radar provides information regarding plant structure and moisture (Government of Canada). A statistical iterative fusion proposed by Melgani and Serpico (2002) showed the fusion of spatial-temporal contextual information with spectral information to classify multi-temporal and multi-sensor images, where absence of parameters makes this fusion interesting compared to other techniques based on MRF's. On the other hand, the use of an MRF based technique for multisource classification has proved to be advantageous since it allows images from different sources and data to be merged in a consistent way, where spatial and temporal context is also readily modeled in the framework (Solberg et al., 1996). Foucher et al. (2002) suggested a different approach in dealing with multisource classification by using Independent component analysis and Dempster-Shafer theory, where Dempster-Shafer rule of combination would enable to fuse decisions in local spatial neighborhood which was then extended to multisource images. Their approach enabled to directly fuse information for the classification of noisy images producing interesting results (Foucher et al., 2002). Jiang et al. (2010) constructed a new classifier integrating multiple sources and multi temporal remote sensing data of wetlands for classification. They have used fuzzy matter element model for constructing an integrated classifier and got an overall accuracy better than SVM results (Jiang et al., 2010). A multi-data approach has been suggested by Waldhoff and Bareth (2009) where they argue that land use data available from official sources lack desired information detail for many purposes like agro-ecosystem modeling. They used Multi-data approach by retrieving information from remote sensing analyses and integrated them into official land use data to enhance both information level i.e. the present land use data and land use classification

(Waldhoff & Bareth, 2009). Amorós-López et al. (2013) stated the potential of proposed spatial un-mixing approach in agricultural monitoring using LANDSAT temporal profiles complemented with MERIS fused images. Monitoring vegetation phenology using MODIS proposed by Xiaoyang Zhang et al. (2003) from time series of satellite data, it shows a method using piece wise logistic functions which are fit to vegetation index data to represent intra-annual vegetation dynamics, using this approach transition dates for vegetation activity within annual time series of VI data can be determined. Wu et al. (2006) studied the land use change dynamics by the combined use of remote sensing and geographic information system. They projected the land-use change for the next 20 years using Markov chain and regression analysis. For understanding the process by which the land use changed they combined Markov chain and regression analyses with GIS and remote sensing (Wu et al., 2006).

2.5. Crop classification using vegetation indices

According to Clevers (1988), reflectance obtained from near infrared is most suitable for estimating leaf area index (LAI) but problem arises if multi-temporal images are used since soil moisture is not constant in different seasons, so Clevers (1988) suggested an approach to calculate corrected infrared reflectance by removing the soil effect which is the weighted difference vegetation index (WDVI). On the other hand, J Qi et al. (1994) suggested that one need to be careful while using WDVI since it is very sensitive to atmospheric variations. According to Huete et al. (1985), soil and plant spectra are partly correlated which produces a composite spectra, so Huete (1988) proposed a method to reduce the soil background effect by introducing a soil adjustment factor L to account for the soil background variations and obtained a soil adjusted vegetation index (SAVI). Baret et al. (1989) proposed a vegetation index based on the similar principles stated by Huete (1988) where the SAIL (Scattering by Arbitrarily Inclined Leaves) model was used to simulate in different conditions the relationship between transformed soil adjusted vegetation index (TSAVI) and leaf area index (LAI), thus TSAVI was defined as the measure of angle between soil line and the line which joins the vegetation point and the intercept of the soil line. J. Qi et al. (1994) stated that using L=0.5 as constant would result in a loss of vegetation dynamic response so for the optimization of L factor in SAVI, prior knowledge of vegetation amounts is required unless one developed an iterative function, this lead them to develop modified soil adjusted vegetation index (MSAVI).

Most of the vegetation indices have concentrated in the visible and near infrared region but there is one more region in the electromagnetic spectrum ranging between 1-3μm which is sensitive to leaf water content because of the absorption of electromagnetic energy in this wavelength. Short wave infrared (SWIR) reflectance decreases as water content in the leaves increases (Gao, 1996; Hardisky et al., 1983; Tucker, 1980). Gao (1996) proposed a new vegetation index for remote sensing of vegetation liquid water which is normalized difference water index (NDWI), this index uses two channels centered near 0.86 μm and 1.24 μm. In principle NDWI is the measure of liquid water molecules in vegetation canopies which are interacted with incoming solar radiation, tests were performed using this index on 2 sets of AVIRIS (Airborne Visible/Infrared Imaging Spectrometer) data which showed that NDWI contains information

independent of NDVI (Gao, 1996). Similarly Jurgens (1997) developed modified NDVI (mNDVI) to determine frost damage in agriculture, the index showed a strong correlation with the plant condition and also with its phenological stages of growth, finally he concluded that the present analysis using mNDVI was only qualitative as detailed statistical reference data was missing in the experiment.

2.6. Object based classification of crops

Increasing number of high resolution images paved path for object oriented classification where objects are aimed to be derived from the pixels encompassing them but on the other hand low resolution and medium resolution images where still the pixels are coarser or as same size that of the object of interest emphasized more on the pixel based and sub-pixel based classification (Blaschke, 2010). According to Benz et al. (2004), the image objects which closely resembles the world objects if derived would contain topological relationships with other objects (e.g., adjacent to, contains, is contained by, etc.), statistical summary of spectral and textural values and shape characteristics which all can be applied for the classification. Liu et al. (2006) presented some important points which are to be kept in mind while working on object oriented remote sensing information classification pattern, they are: 1) developing robust and highly effective image segmentation algorithm; 2) improving the feature-set including edge, spatial-adjacent and temporal characteristics; 3) discussing the classification rule generation classifier based on the decision tree; 4) presenting evaluation methods for classification result by object-oriented classification pattern. In the process of interpreting remote sensing (RS) images, features of land cover play an important role in object based classification of the RS images (Liu et al., 2006). Features are generally divided into three types: spectral, spatial and temporal features but under further elaboration specific features which can be deduced are: hue (color) which reflects the characteristic of land cover feature; size, shape and texture which can be regarded as spatial layout of land cover features; spatial relationship, dynamic change in process and location (Liu et al., 2006).

Some studies such as mapping shrub encroachment using Quick bird imagery (Laliberte et al., 2004), mapping fuel types using LANDSAT TM and IKONOS imagery (Giakoumakis et al., 2002) are interesting. Zhou and Troy (2008) presented an object oriented approach for classifying urban landscape at parcel level by using high resolution digital aerial imagery and LIDAR (Light detection and ranging) data. A three level hierarchical architecture was used where each object was classified differently at different level and finally 92.3 % accuracy was obtained with a kappa statistics of 0.89. Geneletti and Gorte (2003) presented a method for object oriented land cover classification by combining Landsat TM data and aerial photograph. They used a two-step process of sequential segmentation and classification techniques where in the first step they classified the Landsat TM image using maximum likelihood classification and other empirical rules whereas in the second step they segmented the aerial image by applying region based segmentation algorithm and finally by taking the classified Landsat TM image as reference they classified the segmented aerial image (Geneletti & Gorte, 2003). Duro et al. (2012) compared pixel based and object based classification by examining decision tree (DT), random forest (RF)

and support vector machine (SVM). They found that the overall classification accuracies were not statistically significant between pixel based and object based classification produced maps but in object based classification there was a statistically significant difference in classification accuracies between maps produced by DT algorithm compared to SVM or RF algorithms whereas results produced from pixel based image analysis had no statistical significance difference, finally it was concluded that based on overall accuracy reports, there was no advantage of preferring one classification technique over the other for the classification of broad land cover types in agricultural environment using medium spatial resolution imagery (Duro et al., 2012). Esch et al. (2014) proposed a novel method of combining satellite earth observation (EO) data and ancillary geo-information data for the classification of crop land. They used a multi-seasonal high (HR) and medium resolution (MR) imagery for land parcel based determination of crop types and also differentiating between cropland and grassland, based on the derived seasonality index and input imagery cropland and grassland were classified using C5.0 [1]tree classifier, finally the method showed an effective way of classifying different crops and differentiating between cropland and grassland (Esch et al., 2014). Diaz-Varela et al. (2014) presented a novel approach for the classification of agricultural terraces which are complex if they are associated to complex vegetation cover patterns, they have adopted a two stage process where in the first stage, orthoimagery and digital surface models (DSMs) at 11cm spatial resolution are generated using computer vision techniques and then in the second stage these data are used to identify agricultural terraces using multi-scale object oriented method. The automated terrace classification yielded an overall accuracy of 90% based entirely on spectral and elevation data from the imagery (Diaz-Varela et al., 2014). Löw et al. (2013) discussed the impact of feature selection for crop mapping using support vector machine (SVM) at object level and random forest (RF) feature importance score was used to attain optimal accuracy. Their method increased the accuracy by 4.3% and decreased the thematic uncertainty, the uncertainty features of SVM proved to be an important source of information for increasing the overall accuracy (Löw et al., 2013).

[1] A system that extracts informative patterns from the data.

3. DATA DESCRIPTION

3.1. Study area

The present study area is taken around Lauwersmeer Lake in the north of Netherlands because of its typical sea clay soil and wide variety of crops such as potatoes, sugar beet, maize, carrots, onions, winter cereals etc. and with large agricultural fields (Figure 3-1).

Moreover with the introduction of new CAP policy of greening measure, the Ministry of Economic Affairs is showing an interest towards the classification of grasslands in this area.

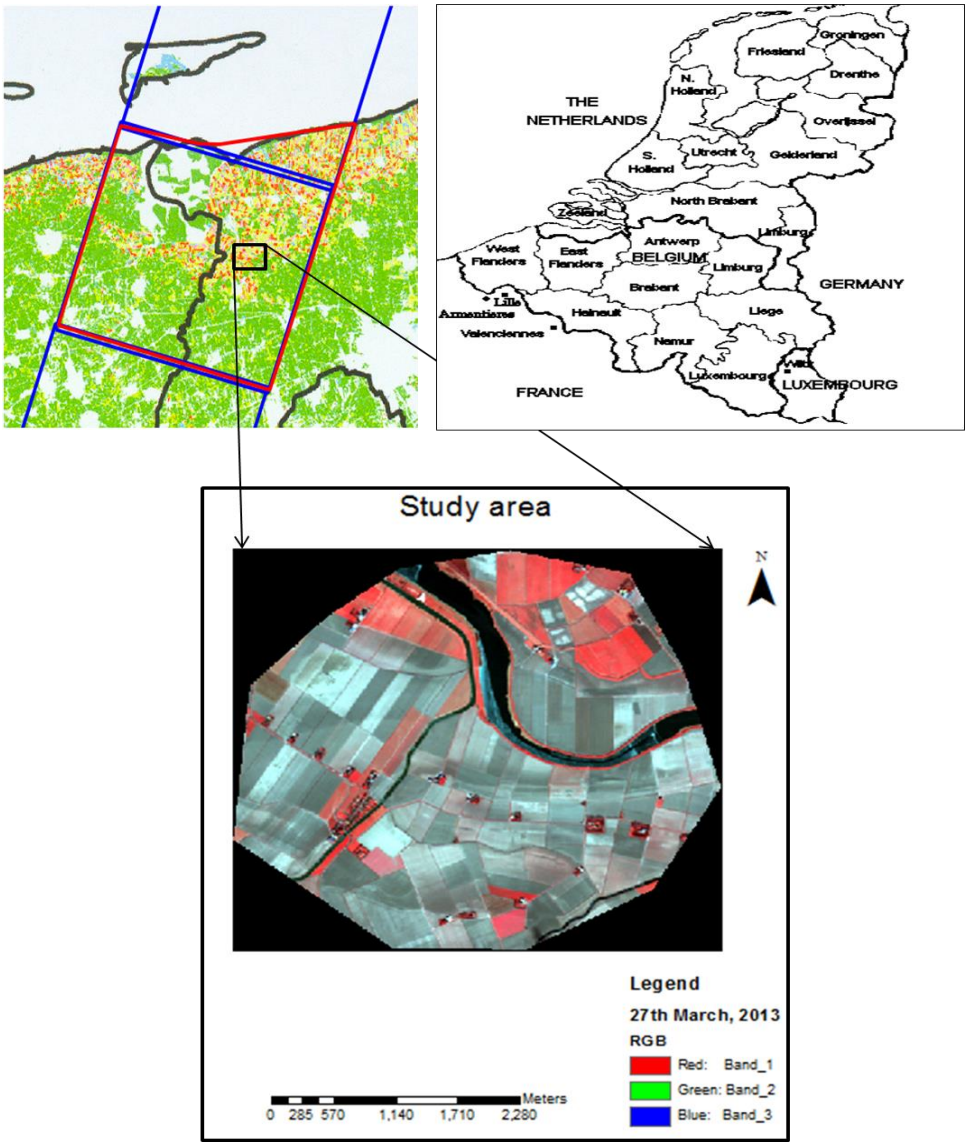

Figure 3-1: Top left image displays the region of interest and the top right displays country "The Netherlands" where in the study area is located. Bottom image displays the study area from the region of interest, it's a SPOT 5 image displayed in false colour composite.

3.2. Data description

The present research has two sets of data comprising of raster and vector datasets acquired in the year 2013. The raster dataset has four multi-sensor images of different dates and vector dataset has a polygon layer of different crop types. The data was provided by NEO Company with permission from Dienst Regelingen (part of Ministry of Economic Affairs).

3.2.1. Multi-sensor datasets

There are four images acquired on different dates of the same year in the area around Lauwersmeer. All the images have been geo-referenced to Double Stereographic projection and Amersfoort (To WGS 84 4) datum. Two images are of Spot 5 (Satellite Pour l'Observation de la Terre) sensors, one image of Spot 6 sensor and one of Pleiades satellite.

Spot 5 images: The two spot 5 images are acquired on dates 27th March and 19th July. The images has red, green, near infra-red and short wave infra-red (SWIR) bands. The band structure of the present images is Band 1 being near infra-red, Band 2 is red, Band 3 green and Band 4 SWIR. The images were geo-referenced when provided, so no image rectification was applied on them.

Spatial resolution is 10m and radiometric resolution is 8bit. The images are shown in false colour composite in Figure 3-2 and Figure 3-3.

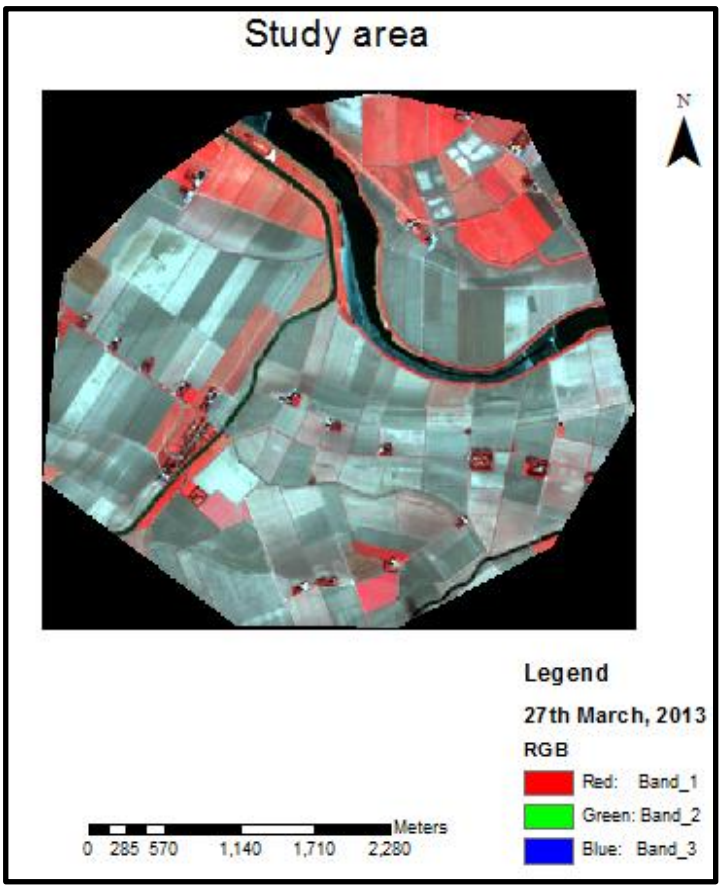

Figure 3-2: 27th March 2013 Spot 5 image. Bands showed here are near infra-red, red and green in a false colour composite combination. The shade of red represents vegetation and cyan represents bare land.

Figure 3-3: 19th July, 2013 Spot 5 image. Bands showed here are near infra-red, red and green in a false colour composite combination. The shade of red represents vegetation and cyan represents bare land.

Spot 6 image: The one spot 6 image was acquired on 2nd June. This image in contrast to spot 5 has a blue band. The band structure of spot 6 is Band 1 being blue, Band 2 is green, Band 3 is red and Band 4 is near infra-red. Spatial resolution of the image is 7mts and radiometric resolution is 16 bit. The radiometric resolution of the image was calibrated for further analysis (refer to section 4.2.2). The image is shown in Figure 3-4.

Figure 3-4: 2nd June 2013 Spot 6 image. Bands showed here are near infra-red, red and green in a false colour composite combination. The shade of red represents vegetation and cyan represents bare land.

Pleiades satellite image: The image was taken on 21st April. It has blue, green, red and near infra-red bands and the band structure is Band 1 blue, Band 2 is green, Band 3 is red and Band 4 is near infra-red. Spatial resolution of the image is 0.5 metres and radiometric resolution is 16bit, the radiometric resolution of the image is calibrated in the analysis. The image is shown in Figure 3-5.

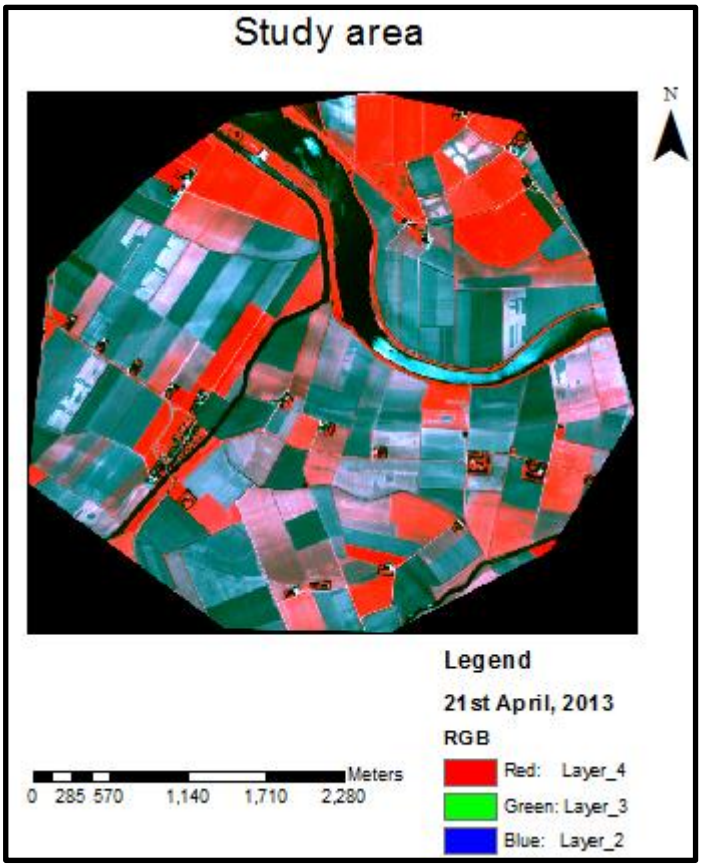

Figure 3-5: 21st April 2013 Pleiades image. Bands showed here are near infra-red, red and green in a false colour composite combination. The shade of red represents vegetation and cyan represents bare land.

3.2.2. Reference data

A vector data having geometry type as polygons was used in this research. The polygons are the agricultural parcels which contains the information about different attribute types like parcel category, parcel type, code of the particular parcel type, perimeter of the parcel, area of the parcel. The projected coordinate system of the vector data is RD New (Rijksdriehoeksmeting) and the projection is "double stereographic".

The vector dataset was used as a reference in the analysis for forming rules, calculating the statistics of parcel of the image under each polygon and finally for the validation of the classification result. The vector dataset is supplied by the farmers in 2012 about what they were planning to grow in 2013. Different crop types are present in the present vector polygon like potatoes, sugar beet, barley, wheat, maize, onions with this grassland permanent, grassland temporary, border wildlife (farmland), open ground vegetables were also included.

Since the present vector dataset was used for accuracy assessment and forming the rules it is been called as reference dataset. The reference dataset has 246 parcels with 14 classes. Table 1 would show all the technical features of the satellite data used in the research.

The vector dataset used as reference data is shown in Figure 3-6.

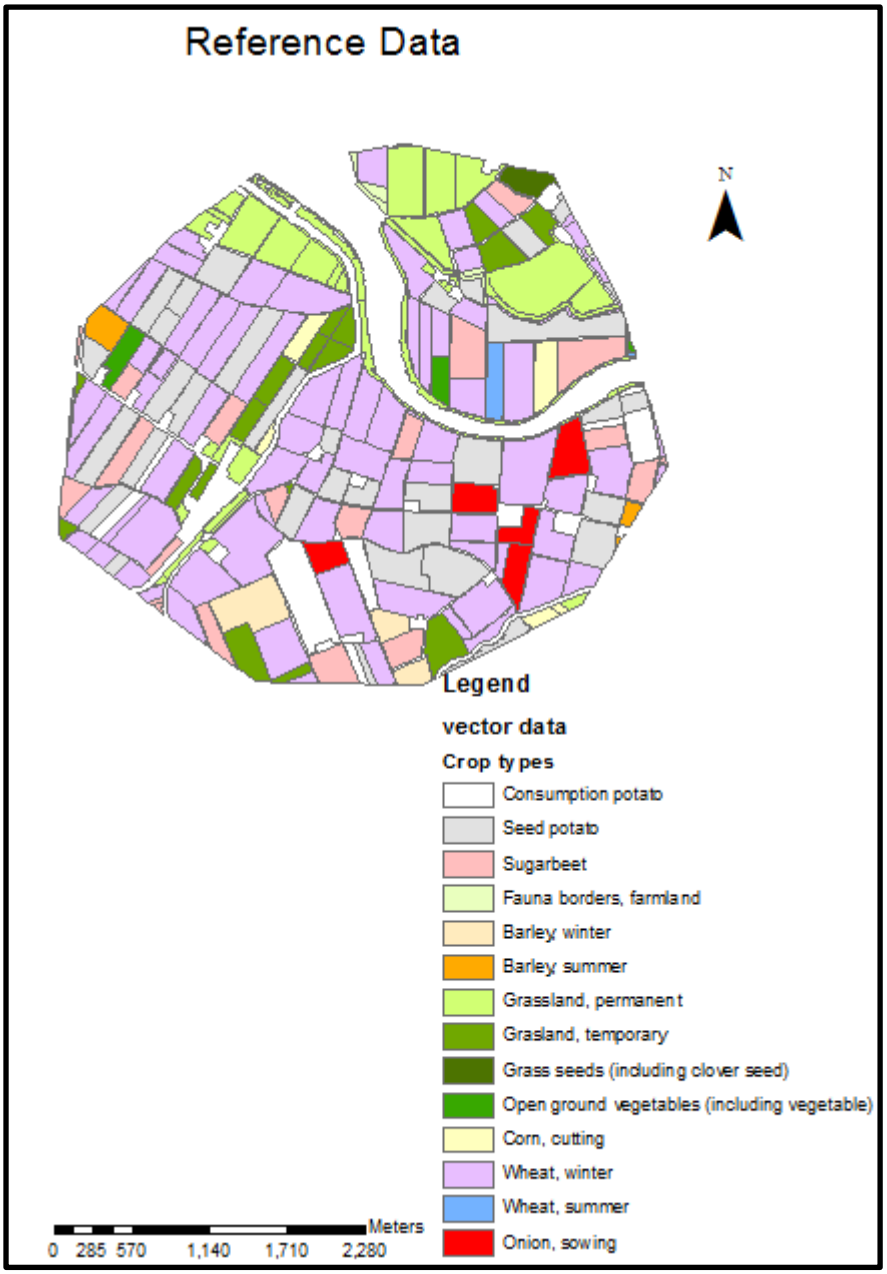

Figure 3-6: Vector data representing crop parcels for the year 2013. There are 14 classes and 246 parcels in the vector dataset.

A table is shown below displaying the technical features of the satellite data used in the research.

Table 3-1: Technical features of the satellite data.

Date of image acquired	Image code	Bands	Spatial resolution	Radiometric resolution	Sun angle (Solar azimuth)	Satellite angle	Name of the satellite
`27th March, 2013	lauw_20130327	B3: Green 0.50 – 0.59 µm B2: Red 0,61 - 0,68 µm B1: Infrared 0,79 - 0,89 µm B4: SWIR 1,58 - 1,75 µm	10m	8 bits/pixel	271.81	98.7°	SPOT 5
21st April, 2013	lauw_east_20130421	B1: Blue: 430-550 nm B2: Green 490-610 nm B3: Red 600-720 nm B4: Near Infrared 750-950 nm	0.5m	12 bits/pixel	278.82	98.2°	Pleiades (satellite)
2nd June, 2013	IMG_SPOT 6_MS	B1: Blue 0.455µm – 0.525µm B2: Red 0.530µm – 0.590µm B3: Green 0.625µm – 0.695µm B4: Near Infrared: 0.760µm – 0.890µm.	7m	12 bits/pixel	285.48	98.2°	SPOT 6

19th July, 2013	lauw_20130719	B3: Green 0.50 – 0.59 μm B2: Red 0.61 – 0.68 μm B1: Infrared 0.79 – 0.89 μm B4: SWIR 1.58 – 1.75 μm	10m	8bits/pixel	282.89	98.7°	SPOT 5

4. METHODOLOGY

4.1. General methodology

The methodology is illustrated in the Figure 4-1. This is the general framework of the research to be used to answer the research questions. There are basically three stages in the proposed methodology that are Data pre-processing, Data Analysis and Crop mapping using rule based classification.

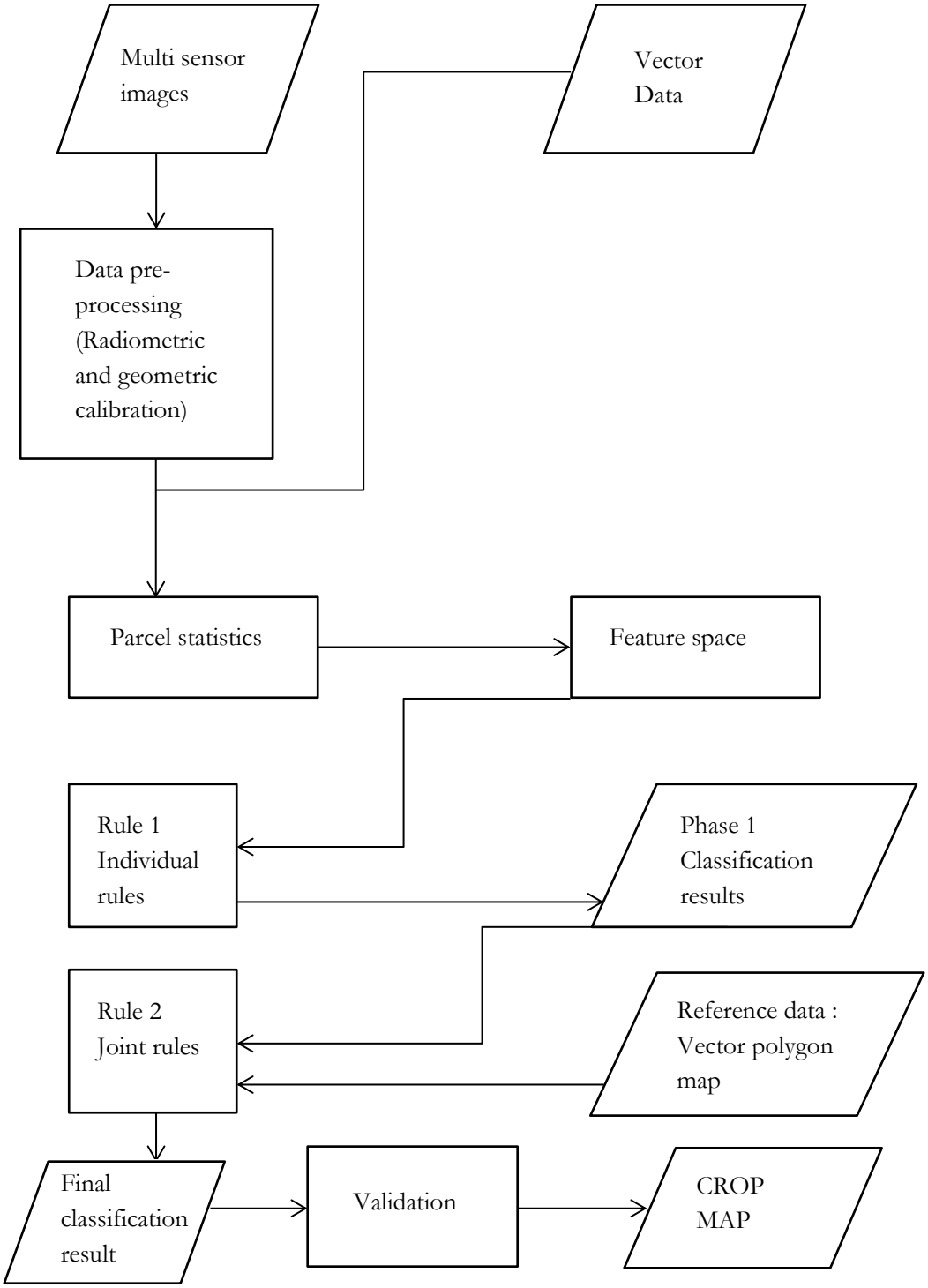

Figure 4-1: General methodology for classifying crop fields using Rule based approach.

4.2. Data pre-processing

The present data for the research was first pre-processed for preparing them before the exploratory analysis. In the raster dataset, out of the four images 2nd June, 2013 SPOT 6 image was not geo-referenced. In the following sections geo-referencing of the 2nd June, 2013 SPOT 6 image and the radiometric calibration of all the images will be discussed.

4.2.1. Geometric transformation

Images are to be rectified in order to have the same projection system so that they can be compared on the same scale. The rectification of the 2nd June, 2013 Spot 6 image was processed in ERDAS imagine through mainly three steps namely; recording the ground control points, computing a transformation matrix and finally resampling the image. 27th March, 2013 Spot 5 image of spatial resolution 10 metres was taken as a reference to rectify Spot 6 image.

The rectification was processed in ERDAS imagine software by first taking the ground control points near the study area and also around the four corners of the image. A polynomial of order 2 was taken as the transformation matrix and finally nearest neighbour method was chosen for resampling as it does not affect the original digital number (DN) values of the pixel. The RMSE error was less than 0.5 pixels, so the image was taken for further analysis.

4.2.2. Radiometric calibration

The ideal result of image pre-processing is to make images appear as if they were acquired from the same sensor (Hall et al., 1991). There are four images with different radiometric resolution. Both the Spot 5 images, 27th March and 19th July have 8 bit radiometric resolution and the other two images of Spot 6 and Pleiades have 12 bit resolution each. All these data were calibrated to bring them on the same platform for further analysis. A table showing satellite images with different radiometric resolutions is shown in Table 4-1.

Table 4-1: Satellite data with their radiometric resolutions.

Date	Satellite	Radiometric resolution
27th March, 2013	SPOT 5	8 bits/pixel
21st April, 2013	Pleiades	12 bits/pixel
2nd June, 2013	SPOT 6	12 bits/pixel
19th July, 2013	SPOT 5	8 bits/pixel

The operation used in the present research for radiometric calibration was the Linear Stretch. The method is used when the input image has narrow histogram or the histogram is close to being uniform (Bakx et al., 2012). Concept behind it is that the digital number (DN) values in the small range having high frequencies of occurrence if stretched between few values in our case between 0 and 255 can provide a normalized and more familiar range that can be distinguished by our senses in much better way if analysed compared to the non-stretched data. The area of interest has the water body which has DN value zero, so in this scenario linear stretching can produce much effective results.

Since the two images of SPOT 6 and Pleiades have 12 bit/pixel radiometric resolution, it was necessary to convert them into 8 bits/pixel resolution as it would bring all images under the same radiometric resolution scale. The process of linear stretching was carried using R software (open platform software). An algorithm was adopted to linearly stretch the image in the desired radiometric resolution, in the algorithm first the image was called which is to be selected and then a function was applied on the image which was inserted, finally a linearly stretched image with a radiometric resolution of 8 bits/pixel was obtained. The function that was used in this case is a linear equation as follows,

$$Y = X \times \frac{255}{1}(maxDN - minDN) \quad (1)$$

where, X= present DN value – minDN value, here DN is Digital number of the pixel and Y is the transformed output of the pixel, minDN is the minimum digital number of a band from all pixels of an image and maxDN is the maximum digital number of a band from all pixels of an image.

All those values which are less than 0 for Y (transformed value) will be assigned 0 and the values which are above 255 will be assigned 255.

The pixel values of the images would be ranging between 0-255 as all the images were transformed into 8 bits/pixel resolution. 8 bits/pixel amounts to 1 byte of data stored so for 4 bands 4 bytes of data is stored compared to 12 bits which is storing 6 bytes of data, by the conversion of data from 12bits/pixel to 8bits/pixel computational speed is increased and made it lot easier to handle higher colour depth images. Also by linear stretching image contrast is improved which would help better in identifying the feature of land parcel in the digital image by applying basic rules of visual interpretation.

By the above analysis four images were obtained linearly stretched into 8 bits/pixel radiometric resolution.

4.3. Data analysis

In the following section images are explored based on their parcel statistics, vegetation indices and the parcels which were plotted in the feature space. According to Liu et al. (2006), land cover features play an important role in object-based classification, some of the specific features used for studying object-based classification are hue or colour, shape, size, texture, spatial relationship and dynamic change in process.

The parcels which were taken in the present analysis are objects since the specific features discussed by Liu et al. (2006) can be obtained. Every parcel is a type of agricultural land with different varieties of crops and every crop has a unique growth period with unique conditions for growth which justifies the crop parcels with different crops to be treated as crops.

4.3.1. Extracting representative pixels

Before obtaining the specific features of objects discussed in the introduction of data analysis (section 4.3), it was very important to first extract the representative pixels of a desired parcel based on which the statistical and specific feature based information of the object can be obtained.

The whole process of extracting pixels of a parcel was carried out in two steps. In the first step the reference data was clipped from the original vector file in the ARCGIS platform. The clipped data was then processed in R software using function to extract the representative pixels. The following function was used to extract the representative pixels.

```
#Read raster image
A <- readGDAL(paste(Path_in,"/",image.fn,".tif",sep=""))
```
(Function 1)

```
# Read vector file
V <- readOGR(paste(Path_in,"/parcel", sep=""), layer=vector.fn)
```
(Function 2)

```
#verifies for one or more points if they fall in a given polygon
point.in.polygon(xy[,1],xy[,2],polxy[,1],polxy[,2])
```
(Function 3)

In Function (1), "readGDAL" calls the raster image, in Function (2) "readOGR" calls the vector file and in the Function (3) "point.in.polygon" verifies whether the pixels of a parcel are inside or outside the polygon, "polxy" represents numerical array of 'xy' coordinates of a polygon.

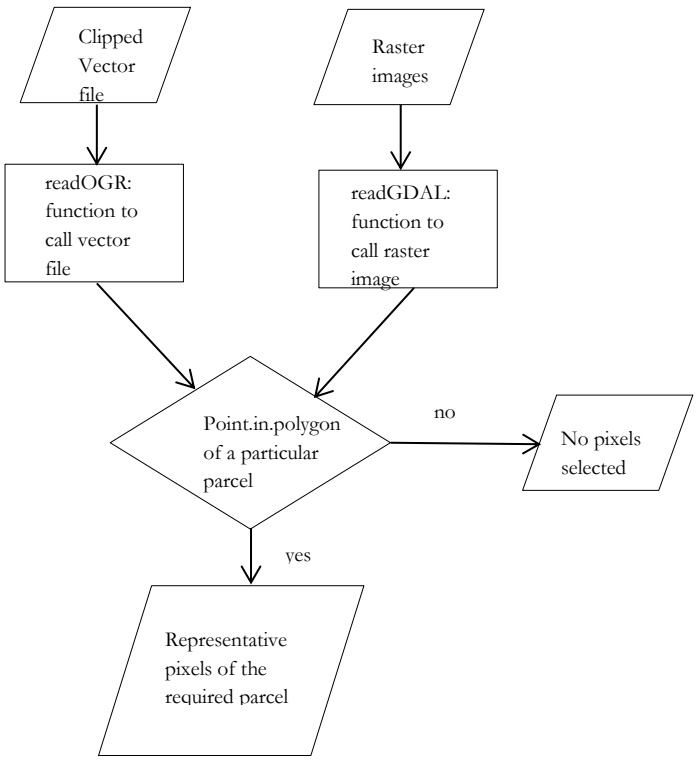

Figure 4-2: Flowchart for the extraction of representative pixels from a parcel.

4.3.2. Parcel statistics

The statistical information present inside the land parcel is an important part of this research. Statistical information taken into account in this research is the mean and the standard deviation of individual bands of the pixels in a parcel of an image.

Mean vector

The position of a pixel in a multispectral space is defined by vectors whose components are the spectral responses in different bands. So, the mean position of the pixels with respect to a particular band can be defined as the mean of all those mean vectors of all pixels of the same particular band. The expected value of the pixel vector is defined as follows (Richards, 2013b),

$$m = \mathrm{E}(x) = \frac{1}{K}\sum_{k=1}^{K} x_k \quad (2)$$

where, m is the mean pixel vector, E is the expectation operator, x_k is the individual pixel vector of total number K

The mean vector of the parcel would show the position of a parcel in a multispectral space. For calculating the mean of different bands of pixels in a parcel, an algorithm was formulated in the R software. The raster layer and the polygon vector layer were both inserted into the code and finally using a "FOR" loop condition, mean values of different bands of pixels in a parcel. All the mean values of different parcels were stored in a ".txt" format.

Standard deviation

In general the variation from the average is called as the standard deviation. A low standard deviation means that the data points are close to mean and high would suggest a spread over large range of values. For the calculation of standard deviation, a covariance matrix was constructed which is defined as follows (Richards, 2013b),

$$C_x = \frac{1}{K-1}\sum_{k=1}^{K}(x_k - \mathrm{m})(x_k - \mathrm{m})^T \quad (3)$$

where, C_x is the covariance matrix, m is the mean pixel vector, x_k is the individual pixel vector of total number K, T is the vector transpose.

Covariance matrix is an important mathematical concept as it deals with the analysis of multispectral data (Richards, 2013b). Further standard deviation was calculated by taking the square root of the diagonal elements in the covariance matrix. The covariance matrix was calculated in the R software for every parcel and then the standard deviation was calculated using the covariance matrix for all the bands. The function used in R software for calculating covariance matrix is given below,

```
Cov[m,,] <- var(y, na.rm = TRUE)
```

(Function 4)

here, y is the data for which covariance matrix is being constructed, var is the function for creating covariance matrix, na.rm represents missing value in R software where in this case TRUE condition would exclude missing values from analysis.

The above Function (1) would create a covariance matrix for a parcel with different bands and the below Function (2) would calculate the standard deviation by taking the square root of the diagonal elements.

```
sd<-sqrt(diag(Cov[m,,]))
```
(Function 5)

here, "diag" represents the diagonal elements and "sqrt" represents the square root.

The variance increases with increase in spatial resolution, as an increase in spatial resolution means an increase in number of pixels which affects the standard deviation and variation of the image.

4.3.3. Vegetation Indices

There are many vegetation indices introduced in the literature like weighted differential vegetation index (WDVI), soil adjusted vegetation index (SAVI), transformed soil adjusted vegetation index (TSAVI), normalized differential vegetation index (NDVI) but in the present research only two indices have been used namely ratio vegetation index (RVI) and normalized vegetation index (NDVI). According to

Ratio vegetation index

Ratio vegetation index (RVI) is defined as the ratio of the reflectance in near infra-red band by red band. The equation is defined as follows (Pearson & Miller, 1972),

$$RVI = \rho_{nir}/\rho_{red} \quad (4)$$

where, ρ_{nir} and ρ_{red} represents reflectance in near infra-red and red bands respectively.

One of the drawbacks in using RVI is that it tends to infinity if reflectance in red band tends to zero (Ünsalan & Boyer, 2011).

RVI was calculated in R software for every parcel and tabulated in the table.

Normalized differential vegetation index

It is defined as the ratio of the difference in reflectance of near infra-red and red band by their sum. The equation is defined as (Rouse et al., 1974),

$$NDVI = (\rho_{nir} - \rho_{red})/(\rho_{nir} + \rho_{red}) \quad (5)$$

where, ρ_{nir} and ρ_{red} represents reflectance in near infra-red and red bands respectively. The NDVI is also calculated in the R software and tabulated.

4.3.4. Feature space

In the present analysis of the data feature space plays an important role in the formation of rules. Feature space is generally prepared to display different observations in the form of a scatter plot and then finally to use their attributes to distinguish them from one another. Since the present research is dealing with the

classification of crop parcels, near infra-red and red bands are taken for forming the feature space as both the bands are very sensitive to vegetation. The mean vector of a parcel in the near infra-red and red bands was plotted in the feature space. In addition to that standard deviations of different parcels for the respective near infra-red and red bands were also plotted.

The feature space helped to spot the cluster and outliers of an individual kind of parcel in the whole image which helped in to study their statistical information and separate them in a group by forming rules. Further in the feature space two different crop types were also displayed to understand the scatter of one crop type with the other one. This helped in making much better classes in the initial phase of classification. Example of a feature space in near infra-red and red bands is shown in Figure 4-3.

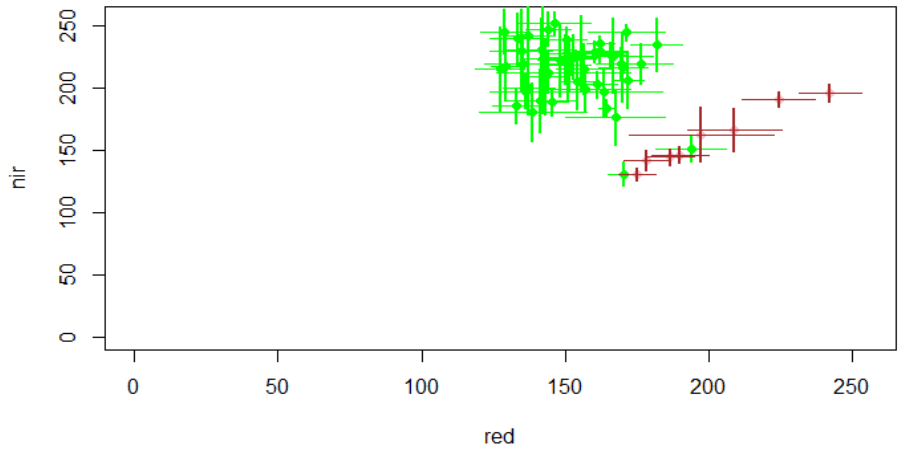

Figure 4-3: A 2D feature space constructed in R software.

This is a 2-dimensional feature space constructed in R software by plotting the mean and standard deviation values of both near infra-red and red bands.

4.4. Rule based classification

Rule based classification is one of the simplest techniques used today and the most common type of rule used is of the form (Richards, 2013a):

If condition **then** inference.

A condition is a logical expression which can either be true or false and if it is true then the condition is said to be justified (Richards, 2013a).

4.4.1. Joint Rule based classification

The present research deals with multi-sensor data so a Joint Rule based approach has been adopted. In this type of rule base approach, every image in the dataset will have its own set of rules and finally the information obtained after the classification would be used for creating a new set of rules for a combined classification to finally produce the desired results.

The basic structure is explained in Figure 4-4 (Richards, 2013a).

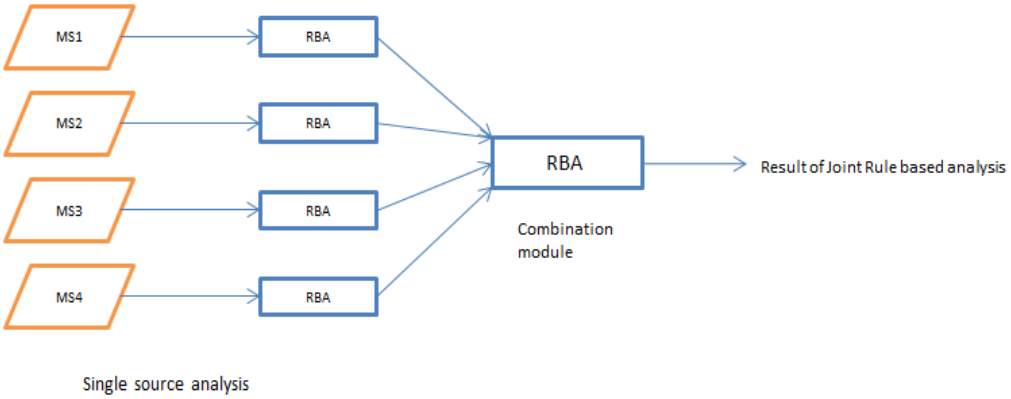

Figure 4-4: Description of Joint rule based analysis, RBA refers to Rule based analysis and MS refers to multi-sensor image.

The classification process in the present research was divided into two parts. First one being the use of feature space of different crop types and form the rules. The second part being the use of the classified parcels of a particular crop type and then train the other parcels using the classes of sample parcels. The advantage of using the joint rule based approach is that more data can be added any time and new parameters can be included in the program if there is a need to refine the model. If there is only one rule base then adding new parameters would be detrimental as the new parameters would behave differently for different sources of data.

A training set was defined for carrying out the object-based rule based classification by taking half the parcels for training and rest for the verification of the results. Out of 246 parcels, 205 parcels of various classes that have to be classified are taken into consideration, only those parcel types have been taken which have more than or equal to 10 parcels, rest of the parcels have not been included for classification or training the algorithm. The training and test set are displayed in Table 4-2.

Table 4-2: Training set and test set of object-based rule-based classification.

Agricultural parcel	Total number of parcels	Training	Verification
Permanent grassland	48	24	24
Temporary grassland	17	8	9
Winter wheat	84	42	42
Seed potato	37	18	19
Sugar beet	19	9	10

4.4.2. First phase of classification

In the first phase of classifying images from different dates, feature space has been used for developing the rules for classification. Vegetation indices like ratio vegetation index (RVI) and normalized differential

vegetation index (NDVI) has also been taken into consideration with the statistical information like mean and standard deviation of near infra-red and red bands for the formation of rules. Different set of rules are formed for different images for classification in the first phase.

The general approach adopted for formation of rules was first by plotting the mean and standard deviation values of different parcels of a particular crop type in near infra-red and red bands. The plotted graph was then analysed based on the outliers and the cluster of points.

Finally training parcels were taken and then based on their statistical information and through visual interpretation, a first set of classes were defined and also the rules to classify them. After the first basic set of rules, this time different crop types were plotted against each other to refine the rules and form much robust classes.

The first type of parcel of an image plotted in the feature space was permanent grassland as they are present in an area throughout the year and through visual image interpretation, the colour of different land parcels on image could easily help in identifying the basic character of a parcel if it is vegetation or bare land. By analysing the feature space, the first observation of analysis taken were the outliers where mean and standard deviation of the particular outlier was analysed and through visual interpretation in false colour composite a class was assigned to them. Using this strategy the next point of observation were the parcels in clusters, they too were analysed in the same process and classes were assigned. After this different crop types were plotted against the grassland permanent to analyse if there are some parcels which exist between the outlier and cluster of grassland permanent parcel, if yes the same discussed steps for analysis were applied on them and new classes were formed.

In the first phase of classification as discussed, feature space of grassland permanent parcels were plotted first and then later other crop types were plotted against it. Thus feature space showed the parcels on which rules were formed to classify them.

Since separate rules were formed for different images, each rule base would be discussed and results will be displayed. The classes which were classified in the first phase of classification for different images are given below.

a. **Mixed parcel**: Mixed parcel are those parcels whose some proportion of parcel land is bare land or vegetation. So, after observing some parcels in the image, those parcels whose standard deviation was much higher compared to the other parcels were taken into account and used for training the other parcels having same character. Total number of parcels classified was 12 out of 246 after applying the rule on the image.

b. **Bare land**: For this first the grassland permanent was taken into account and the parcels which are outliers were studied with respect to the fact that most of the parcels of grassland permanent should have some vegetation. These outlier parcels were studied which showed that their value in red band is much higher than their value in near infra-red region which inclines towards the reason that bare land reflects more red band than and very less near infra-red. After this other

crop types were also plotted in the feature space against the grassland permanent and those parcels of these crop types which were close to the outliers and in the same line to the outliers of grassland permanent were studied. Even those parcels showed similar characteristics like that of outliers of grassland permanent. Finally, some of these parcels were taken and NDVI was calculated, which was less than zero in all the selected parcels. These selected parcels were used as training sample to classify all other parcels having the same characteristics. Total number of parcels classified was 175 out of 246 as bare lands.

c. **Uniform sparse vegetation**: For the classification of uniform sparse land same process was applied like explained in the case of bare land but here the case of uniformity is taken into account to separate even mildly vegetated ground from uneven vegetated ground. For this case standard deviation has been taken into account as it can clearly define the variability existing in the field. Through visual interpretation 15 was taken as the threshold of standard deviation in both near infra-red and red bands to separate such fields. Parcels classified were 11 out of 246.

d. **Non-uniform sparse vegetation**: It is simple those parcels whose standard deviation was more than 15 threshold in both the near infra-red and red bands. Parcels classified were 4 out of 246.

e. **Uniform normal vegetation**: Using the same approach discussed earlier, those parcels in grassland permanent were studied whose mean values in near infra-red band was higher compared to red band. Also the selected parcels showed their normalized differential index values were ranged between 0.1-0.2. So these selected parcels were used as the training sample for classifying similar parcels. Parcels classified were 12 out of 246.

f. **Non-uniform normal vegetation**: Only the threshold limit was removed. Parcels classified were 20.

g. **Dense vegetation**: Through the feature space some mean band values having very high near infra-red and very less red band mean values can be spot. For such parcels normalized differential vegetation index was calculated and showed they were ranging between 0.2-0.4 and so by taking these sample parcels dense vegetated parcels were classified. Numbers of parcel classified as dense vegetation were 12 out of 246.

h. **Non-uniform dense vegetation**: Threshold limit of standard deviation is removed for the classification into non uniform dense vegetation. Numbers of parcel classified as non-uniform dense vegetation were 32.

A table displaying the rules developed for classifying 27th March, 2013 SPOT 5 image is given below in Table 4-3.

Table 4-3: Rules for classifying 27th March, 2013 SPOT 5 image.

Image	Classification class	Rule
27th March, 2013 SPOT 5	Mixed parcel	**((SD near infra-red>30)OR(SD red>30))**
	Bare land	**(NDVI<0)**
	Uniform sparse vegetation	**(((NDVI>0)AND(NDVI<0.1)) AND ((SD near-infrared<15)AND(SD red<15)))**
	Non-uniform sparse vegetation	**((NDVI>0) AND (NDVI<0.1))**
	Uniform normal vegetation	**(((NDVI>0.1)AND(NDVI<0.2))AND((SD near-infrared<15)AND(SD red<15)))**
	Non-uniform normal vegetation	**((NDVI>0.1) AND(NDVI<0.2))**
	Dense vegetation	**((NDVI>0.2) AND(NDVI<0.4))**

A new class has been added here that is the very mild vegetation as there were some parcels where a slight growth of vegetation is spotted and image being a very high resolution image could spot such change. The rules for classifying this image are:

a. **Mixed parcel**: The process described earlier was applied here and after the analysis standard deviation of 35 for both the near infra-red and red bands was taken as the threshold for classifying mixed parcels. Numbers of parcel classified as mixed parcel were 20.

b. **Bare land**: Ratio vegetation index (RVI) was used as the parameter to separate the parcels. The use of RVI instead of NDVI was due to the reason that the feature space of NDVI for all parcels was concentrated between -0.5 to 0.5, which made the NDVI values concentrated. The RVI values of the parcels in the feature space were ranging between 0-2 so making it easier to separate different parcels, RVI was taken into consideration. The same method was applied as discussed earlier differentiating bare land. Numbers of parcel classified as bare land were 143.

c. **Very mild vegetation**: There were some parcels near to bare land parcels in the feature space. These parcels have mean values of near infra-red and red bands close to each other, so for this

reason a new class was formed which shows very mild vegetation something ranging between sparse vegetation and bare land. Numbers of parcel classified as very mild vegetation were 16.

d. **Uniform sparse vegetation**: It is slightly more vegetated than very mild vegetation so for the classification of uniform sparse land parcels, same process was applied like explained for the previous image. Numbers of parcel classified as uniform sparse vegetation were 8.

e. **Non-uniform sparse vegetation**: After analysing the training sample parcels whose threshold of standard deviation were more than 15 in both the near infra-red and red bands such parcels were classified as non-uniform sparse vegetation. Numbers of parcel classified as non-uniform sparse vegetation were 9.

f. **Uniform normal vegetation**: After analysing the training sample parcels, the parcels whose ratio vegetation index (RVI) was between 0.8 and 1.2 and whose threshold of standard deviation is less than 15 were classified as uniform normal vegetation. Numbers of parcel classified as uniform normal vegetation were 6.

g. **Non-uniform normal vegetation**: After analysing the training sample parcels, the parcels whose ratio vegetation index (RVI) was between 0.8 and 1.2, such parcels were classified as uniform normal vegetation. Numbers of parcel classified as non- uniform normal vegetation are 17.

h. **Dense vegetation**: For training parcels whose RVI is greater than 1.2 were used to classify the rest of the parcels as dense vegetation. Numbers of parcel classified as dense vegetation were 27

Table 4-4: Rules for classifying 21st April, 2013 Pleiades image.

Image	Classification class	Rule
21st April, 2013 PLEIDES	Mixed parcel	**((SD near infra-red > 35) OR (SD red > 35))**
	Bare land	**(RVI<0.65)**
	Very mild vegetation	**((RVI<0.7) AND (RVI >0.65))**
	Uniform sparse vegetation	**(((RVI >0.7) AND (RVI <0.9)) AND ((SD near infrared<15) AND (SD red<15)))**
	Non-uniform sparse vegetation	**((RVI >0.7) AND (RVI <0.9))**
	Uniform normal vegetation	**(((RVI >0.8) AND(RVI <1.2))AND((SD near infrared<15)AND(SD red<15))**
	Non-uniform normal vegetation	**((RVI >0.8) AND(RVI <1.2))**

Dense vegetation	**(RVI >1.2)**

Moving on to the 2nd June, 2013 image, similar analysis has been performed on it as discussed in the earlier images. The uniform and non-uniform parcel clause which defines the evenness of pixels in the parcels has not been included in the rules formation as in the feature space most of the parcels had high standard deviations in both near infra-red and red bands. The classes defined for the image are mixed parcel, bare land, sparse vegetation, normal vegetation, dense vegetation. The rules defined for the classes are:

a. **Mixed parcel**: Applying the previous discussed approach, it was found that the threshold of standard deviation was taken 40 for near infra-red and red bands of different parcels. Numbers of parcel classified as mixed parcels were 52.

b. **Bare land**: Normalized differential vegetation index (NDVI) was taken as the parameter for classifying as discussed earlier the outliers of grassland permanent parcel showed NDVI less than zero. After analysing the feature space of different crop type parcels, NDVI parameter was used and rule was made out of it for classifying bare land. Numbers of parcel classified as bare land were 61.

c. **Sparse vegetation**: Parcels slightly above the bare land in the feature space were analysed which formed the rule for classifying the sparse vegetation parcels. Numbers of parcel classified as sparse vegetation were 25.

d. **Normal vegetation**: The parcels in the feature space having high near infra-red and less red band mean values were taken into account for analysis. These parcels had NDVI between 0.4-0.7 and there were some more parcels above these having very high near infra-red and greater NDVI than 0.7. So, the parcels in the range 0.4-0.7 were taken as the normal vegetation class. Numbers of parcel classified as normal vegetation were 45.

e. **Dense vegetation**: The parcels which were having very high near infra-red mean value and very less red band mean value were taken into account. Ratio vegetation index was increasing infinitely for these types of parcels, so for this reason normalized differential index (NDVI) was taken as it is known that NDVI range from -1 to 1. Finally after analysing the training sample parcels an NDVI of greater than 0.7 was taken for classifying the parcels as dense vegetation. Numbers of parcel classified as dense vegetation were 63.

Table 4-5: Rules for classifying 2nd June, 2013 SPOT 6 image.

Image	Classification class	Rule
2nd JUNE, 2013 SPOT 6	Mixed parcel	**((SD near infrared>40) AND (SD red>40))**
	Bare land	**(NDVI<0)**
	Sparse vegetation	**((NDVI <0.4)AND(NDVI >0))**
	Normal vegetation	**((NDVI >0.4) AND(NDVI <0.7))**
	Dense vegetation	**((NDVI >0.7))**

For the 19th July image, the parcels which were plotted against each other showed that most of the parcels were having higher near infrared and lower red values. Visual interpretation of the training parcels showed that most of the parcels were in red colour in false colour composite. More classes were made under vegetation as most of the training parcels were vegetated or slightly vegetated.

The rules for the classification of 19th July, 2013 SPOT 5 image are given below:

a. **Mixed parcel**: Based on the analysis of training parcels in feature space, the parcels whose standard deviation in near infra-red and red bands was greater than 40 were classified as mixed parcels. Number of parcels classified as mixed parcels were 16 out of 246.

b. **Bare land**: Based on the normalized differential vegetation index (NDVI) feature space of all the training parcels and the feature space of training parcels of different crops in near infrared and red band, it was noticed that the crop parcels as outliers which are having an NDVI of less than zero, such outliers were used as training sample to train other parcels. Numbers of parcels classified as bare land were 8.

c. **Uniform sparse vegetation**: For the classification of uniform sparse vegetation parcel same process was applied like explained in the case of bare land but here the case of uniformity is taken into account to separate even mildly vegetated ground from uneven vegetated ground. For this case standard deviation was taken as it can clearly define the variability existing in the field. Through visual interpretation 15 was taken as the threshold of standard deviation in both near infra-red and red bands to separate such fields. Number of parcels classified as uniform sparse vegetation was 10.

d. **Non-uniform sparse vegetation**: The training parcels whose standard deviation was more than 15 in both the near infrared and red bands. Numbers of classified parcel as non-uniform sparse vegetation were 13.

e. **Uniform normal vegetation**: Using the same approach discussed earlier, those training parcels in whose mean values in near infra-red band was higher compared to red band. Also the selected parcels showed their normalized differential index (NDVI) values were ranged between 0.1-0.3. So, these selected parcels were used as the training sample for classifying similar parcels. Parcels classified were 93.

f. **Non-uniform normal vegetation**: Only the threshold limit was removed. Parcels classified as non-uniform vegetation were 44.

g. **Uniform dense vegetation**: Through the feature space some mean band values having very high near infra-red and very less red band mean values can be spot. For such parcels normalized NDVI was calculated and showed they were ranging above 0.3 and so by taking these sample parcels dense vegetated parcels were classified. Numbers of parcel classified as uniform dense vegetation were 30.

h. **Non-uniform dense vegetation**: Threshold limit of standard deviation was removed for the classification into non uniform dense vegetation. Numbers of parcel classified as non-uniform dense vegetation were 32

Table 4-6: Rules for classifying 19th July, 2013 SPOT 5 image.

Image	Classification class	Rule
19th July, 2013 SPOT 5	Mixed parcel	**((SD near infrared>30)OR(SD red>30))**
	Bare land	**(NDVI <0)**
	Uniform sparse vegetation	**(((NDVI >0) AND(NDVI <0.1))AND((SD near infrared<15)AND(SD red<15)))**
	Non-uniform sparse vegetation	**((NDVI >0) AND (NDVI <0.1))**
	Uniform normal vegetation	**(((NDVI >0.1)AND(NDVI <0.3))AND((SD near infrared<15) AND (SD red<15)))**
	Non-uniform normal vegetation	**((NDVI >0.1) AND(NDVI <0.3))**
	Uniform dense	**((NDVI >0.3)AND((SD near infrared<15) AND (SD red<15)))**

vegetation	
Non-uniform	**((NDVI >0.3))**
Dense vegetation	

4.4.3. Final phase of classification

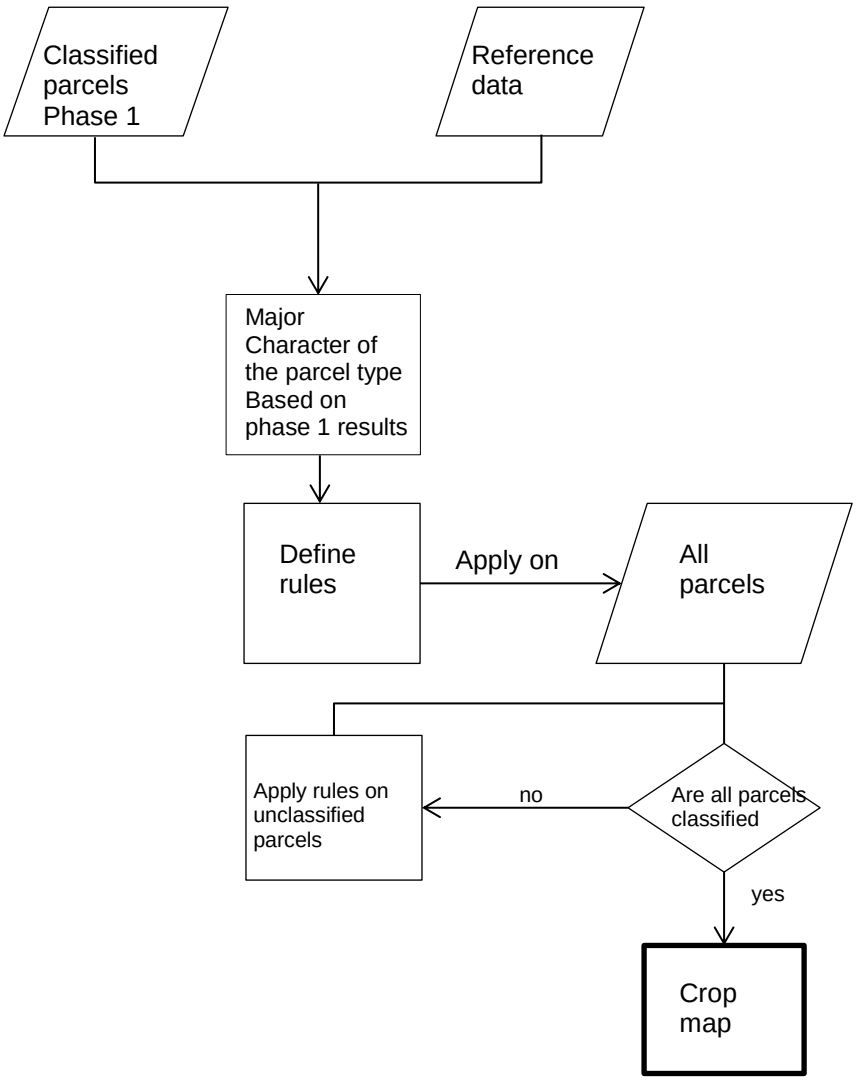

Figure 4-5: Displays the detailed classification steps for Phase 2.

In the final phase of classification different crop types have to be classified. The approach adopted was to take sample of parcels of a particular crop type and then analyse their newly formed classes which were formed in the first phase of classification.

Based on the analysis of a particular set of classes (formed in the first phase of classification), a specific set of classes were made to classify that particular crop type.

The logic behind the classification was applied in R software using "which" operator. In this type of operation, the order of applying rule of a certain class for classification is important. Starting with the mixed parcels, all those parcels whose parcels were mixed in any one of the image have been taken out.

The mixed parcels are those parcels which have both vegetation and bare land in some proportion in the parcel. An example of mixed parcel is shown in Figure 4-6.

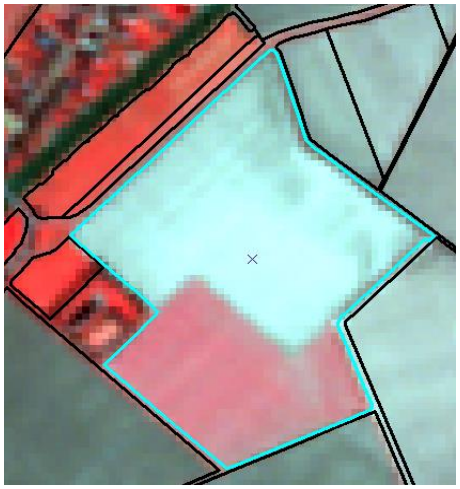

Figure 4-6: In the present image highlighted polygon is the mixed parcel.

Such parcels have to be eliminated as they would add confusion in classifying different parcel types. After the classification of mixed parcels and before classifying the final parcel types, a table was prepared which gave the data about the number of parcels of a particular type in a particular date and for a particular class type classified in the first phase of classification. Based on this data rules were developed for individual parcel type based on the majority of parcels for a class type from the first classification result. For example, a particular parcel type has different number of parcels for different class type obtained from first classification result; the class type which has comparatively highest number of parcels was taken as the characteristic of that parcel type for a specific date. The characteristics of other parcel types are obtained from the same method and then those parcel types having same characteristics are then analysed in other images till a rule is formed to differentiate every parcel type from one another.

The first classification class taken was permanent grassland. Looking at the number of parcels of 27th March image, a characteristic of bare land was seen with most of the parcel types thus showing vegetation only for temporary and permanent grassland. Since bare land was common for majority of crop types on 27th March, other characteristics like uniform sparse vegetation and uniform normal vegetation were also looked upon, as matter of fact normal to dense vegetation was common in permanent grassland it was taken as a condition to separate them from temporary grassland which were more in the range of sparse to normal vegetation.

In the same fashion, the temporary grassland was classified from rest of the parcels since its major characteristic was ranging between ranges of sparse to normal vegetation throughout all the images. All the types of vegetation showed some characteristic in different dates for temporary grassland except the bare land. This easily helped to distinguish it from other crop types since all of them have bare land characteristic in the 27th march image.

Sugar beet was classified after permanent grassland. There were 19 parcels in the reference data from which 9 were taken to train the sugar beet class. This was done by first selecting the majority class type

based on number of parcels which was bare land for 27th March and 21st April, dense vegetation for the 2nd June and ranging between uniform normal vegetation to uniform dense vegetation for the 19th July image which means according to Meier (1997), seeds undergo transformation into fully harvestable plants according to the primary and secondary principles.

Next classified parcel type was wheat winter. Wheat winter showed a strong degree of bare land character in the first two images of 27th March & 21st April and a vegetation character in the 2nd June image with a strong vegetation character in the 19th July, so keeping in mind the principal of growth proposed by Meier (1997).

After that seed potato was classified which showed similar characteristic like that of sugar beet for the first two dates but there was a transformation when it came to the 2nd June image where it was normal vegetation. In the 19th July image the majority characteristic was ranging between uniform normal vegetation to uniform dense vegetation.

A table is shown displaying the rules applied for the classification of different parcel types. A "which" logical operator was used in a specific order and the program was run in such a manner as if once a parcel got a class id then again the next rule won't be applied on it. Only those parcels which are not classified would entertain a rule and of the classified parcels would be left unchanged.

Table 4-7: Rules shown for different classes. All the rules were applied in a specific order as displayed in the table.

Type of parcel	Rules	Order
Temporary grassland	`which((Crop@data$crop_type==0)` `&((P1@data$class_id==2)|(P1@data$class_id==3)\|` `(P1@data$class_id==5)|(P1@data$class_id==6))` `&((P2@data$class_id==6)|(P2@data$class_id==7)\|(P2@data$class_id==8))` `&((P3@data$class_id==3)\|(P3@data$class_id==4))` `&((P4@data$class_id==3)\|(P4@data$class_id==5)|` `(P4@data$class_id==6)\|(P4@data$class_id==7)))`	3
Permanent grassland	`which((Crop@data$crop_type==0)&((P1@data$class_id==3)|` `(P1@data$class_id==4)\|(P1@data$class_id==5)` `|(P1@data$class_id==6)\|(P1@data$class_id==7))&` `((P2@data$class_id==7)\|(P2@data$class_id==8))&` `((P3@data$class_id==2)\|(P3@data$class_id==3)|` `(P3@data$class_id==4)\|(P3@data$class_id==5))&` `((P4@data$class_id==4)\|(P4@data$class_id==5)|` `(P4@data$class_id==6)\|(P4@data$class_id==7)))`	2
Sugar beet	`which((Crop@data$crop_type==0)` `&((P1@data$class_id==2))` `&((P2@data$class_id==2))` `&((P3@data$class_id==2)|(P3@data$class_id==5))` `&((P4@data$class_id==5)|(P4@data$class_id==7)\|` `(P4@data$class_id==8)))`	4
Seed	`which((Crop@data$crop_type==0)` `&((P1@data$class_id==2))`	5

potato	&((P2@data$class_id==2)) &((P3@data$class_id==4)|(P3@data$class_id==5)) &((P4@data$class_id==5)|(P4@data$class_id==7)))	
Wheat winter	which((Crop@data$crop_type==0) &((P1@data$class_id==2)) &((P2@data$class_id==2)\|(P2@data$class_id==5)) &((P3@data$class_id==2)\|(P3@data$class_id==4)| (P3@data$class_id==5)) &((P4@data$class_id==6)|(P4@data$class_id==7)\| (P4@data$class_id==8)))	6
Mixed parcel	which(((P1@data$class_id==1))\| ((P2@data$class_id==1))| ((P3@data$class_id==1))\| ((P4@data$class_id==1)))	1

4.5. Accuracy assessment

The accuracy assessment would be done by creating an error matrix. The reference vector data would be used for the accuracy assessment as half the samples would be taken for training the data and the rest would be used for the accuracy assessment.

4.6. Software and packages

The software and packages used for the analysis have been tabled in Table 3.

Table 4-8: Software used in the research.

Software	Package	Description
R	rgdal	For handling shape files and reference system transformations
	maptools	Handling point, line and polygon
	raster	For creating raster layer objects
	rgl	Multiple devices are managed
ARCGIS	Spatial Analyst	For subset study area region
MS Excel		Handling text files Used for plotting data
ERDAS Imagine	Geometric calibration	Geo-referencing

5. RESULTS

5.1. Data pre-processing

Using geometric transformation 2nd June, 2013 image was rectified. The radiometric calibration of all the images was performed in R software. The results showing the histogram for different dates are shown in Figure 5-1.

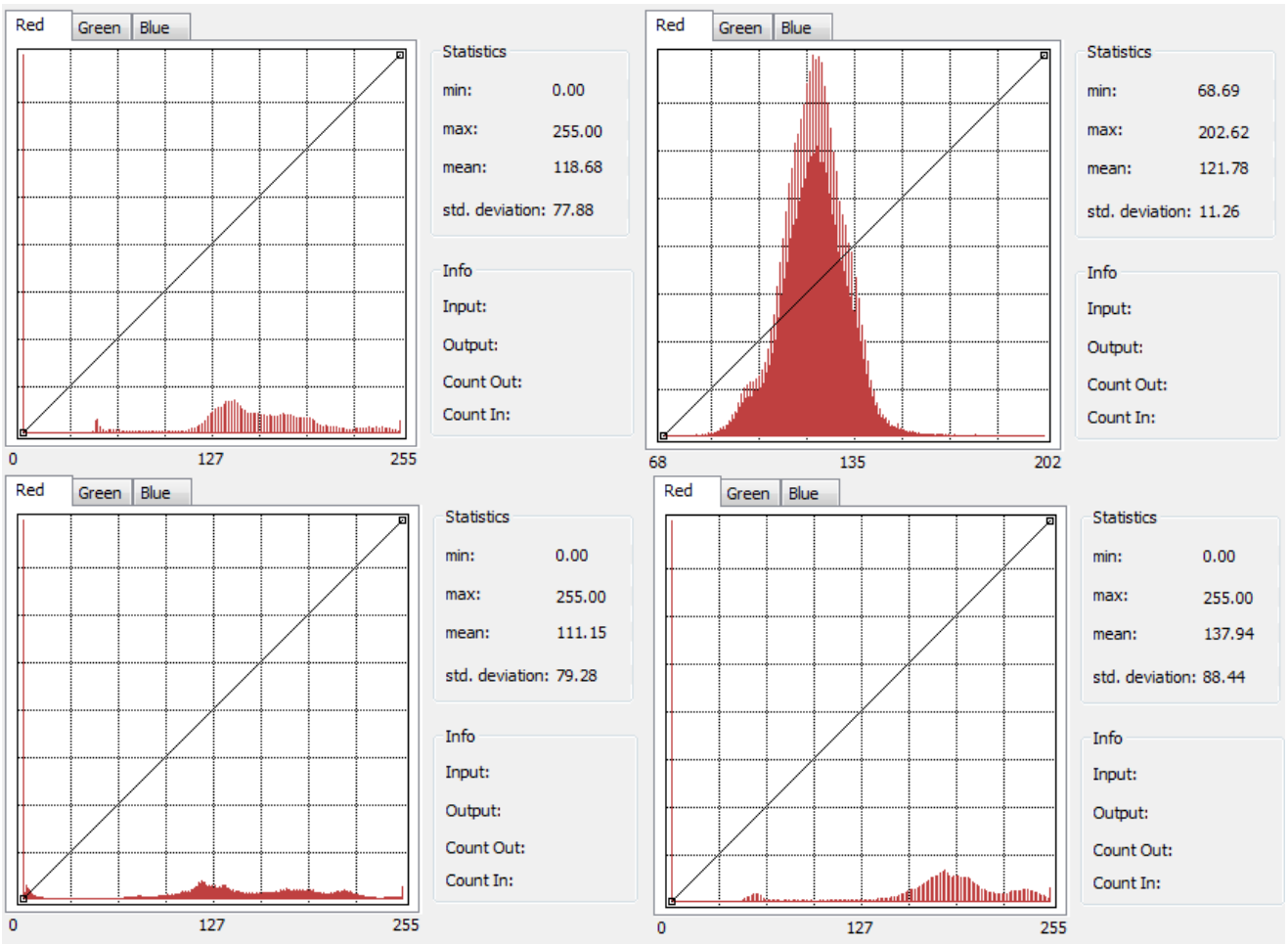

Figure 5-1: Histograms of linearly stretched images are displayed above. Top left is 27th March, 2013 image, top right is 21st April, 2013 Pleiades image, bottom left is 2nd June, 2013 SPOT 6 image and bottom right is 19th July, 2013 SPOT 5 image.

5.2. Data analysis

5.2.1. Parcel statistics and vegetation index

The parcel statistics of all the images was calculated in R software. The main statistics taken in the study are mean and standard deviation of near infra-red and red bands. Figure 5-2 shows parcel statistics and vegetation indices of some of the parcels of 21st April.

class_id	mu1	mu2	mu3/red	mu4/nir	sd1	sd2	sd3	sd4	vi	ndvi	object_id
8	101.342218	145.022776	160.16249	211.227317	11.3919577	7.10458489	6.43647498	24.9728386	1.31883138	0.137496577	1
8	102.94897	145.737806	159.896284	209.501543	10.8262532	7.15457905	6.08651646	9.69788798	1.31023397	0.134286819	2
12	163.272939	174.453249	191.172175	88.5902135	8.59196833	6.62926004	5.72535838	8.03406408	0.46340538	-0.366675313	3
12	161.103219	176.916548	190.011161	110.39152	7.834549	5.98324833	5.06184121	9.5142904	0.58097387	-0.265043043	4
12	141.093514	169.930437	181.466182	150.472876	9.87321498	5.97056667	5.42345047	15.4971136	0.82920616	-0.09337047	5
12	167.574139	188.027835	196.381214	141.855345	23.8884058	17.2978507	14.5769402	16.1460258	0.72234681	-0.161206316	6
12	203.920145	209.931794	215.65921	121.309593	17.5589891	16.4145186	12.9037932	15.7476706	0.56250597	-0.279995109	7
6	158.94772	171.429727	187.6822	92.9774803	7.68863187	5.71558068	5.09568526	12.6131089	0.4953985	-0.337436142	8
6	179.848505	194.33296	202.71337	125.764982	16.7026421	11.5144114	9.33419827	9.61683186	0.62040793	-0.234257106	9
2	209.515919	222.928548	223.461631	147.326627	19.0548464	13.5113348	11.43691	10.17954	0.65929272	-0.205332834	10
1	200.759674	220.05121	218.32527	155.683752	25.5793221	18.6767866	15.9041194	11.8205907	0.71308169	-0.167486649	11
1	200.751149	211.642464	218.108909	129.729401	16.7330722	14.7616592	10.8280111	18.7664976	0.59479185	-0.254082158	12
3	178.110438	184.658736	196.794536	97.910687	10.7218109	9.17812517	7.53467995	7.41652673	0.49752747	-0.33553477	13
10	184.832903	193.386865	207.125077	95.7387649	12.3522056	9.30603822	7.80235053	9.77799911	0.46222682	-0.367776858	14
12	191.1389	196.734708	209.036323	100.182641	7.88203222	5.57271414	5.12346405	7.10227357	0.47925949	-0.352027832	15
3	179.919558	190.364117	199.85788	115.881123	10.5464705	7.28913224	6.17512396	5.76462712	0.57981763	-0.265968907	16
1	161.657184	176.971998	189.41119	123.822447	6.78149364	5.88735877	4.73957737	7.23495591	0.65372297	-0.209392402	17
13	173.505823	185.064886	199.577122	95.8401789	13.820307	10.8078438	9.96582109	17.8265612	0.48021626	-0.351153919	18

Figure 5-2: Displays the parcel statistics of 21st April, 2013.

Here "mu" represents the mean of a parcel for a particular band and "SD" is the standard deviation. Object id represents the parcel number and class id is the type of parcel. "VI" is the ratio vegetation index and "NDVI" is the normalized differential vegetation index.

5.2.2. Feature space

Feature space plots of different parcels are made for different images. Parcels of permanent grassland were plotted and then the other crop types were plotted in comparison to permanent grassland.

Feature spaces of different images are shown from Figure 5-3 to Figure 5-6.

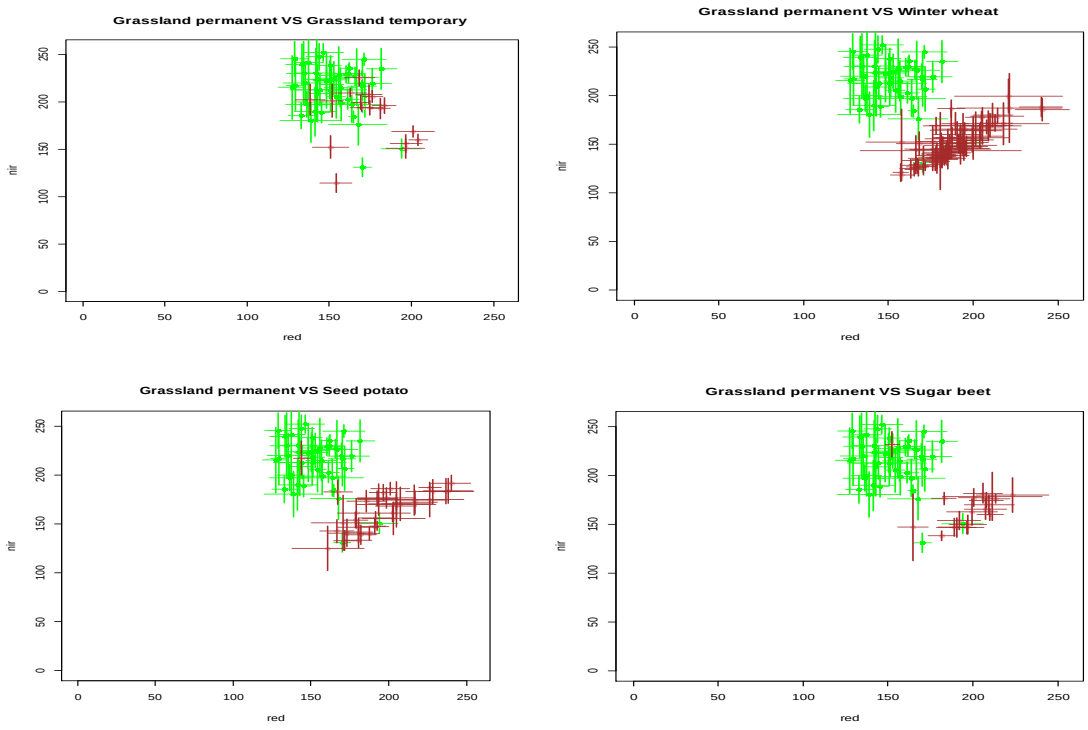

Figure 5-3: Feature spaces of 27th March, 2013 are displayed. Green indicates grassland permanent parcels with their standard deviations represented by lines. Brown indicates grassland temporary in top left, winter wheat in top right, seed potato in bottom left and sugar beet in bottom right.

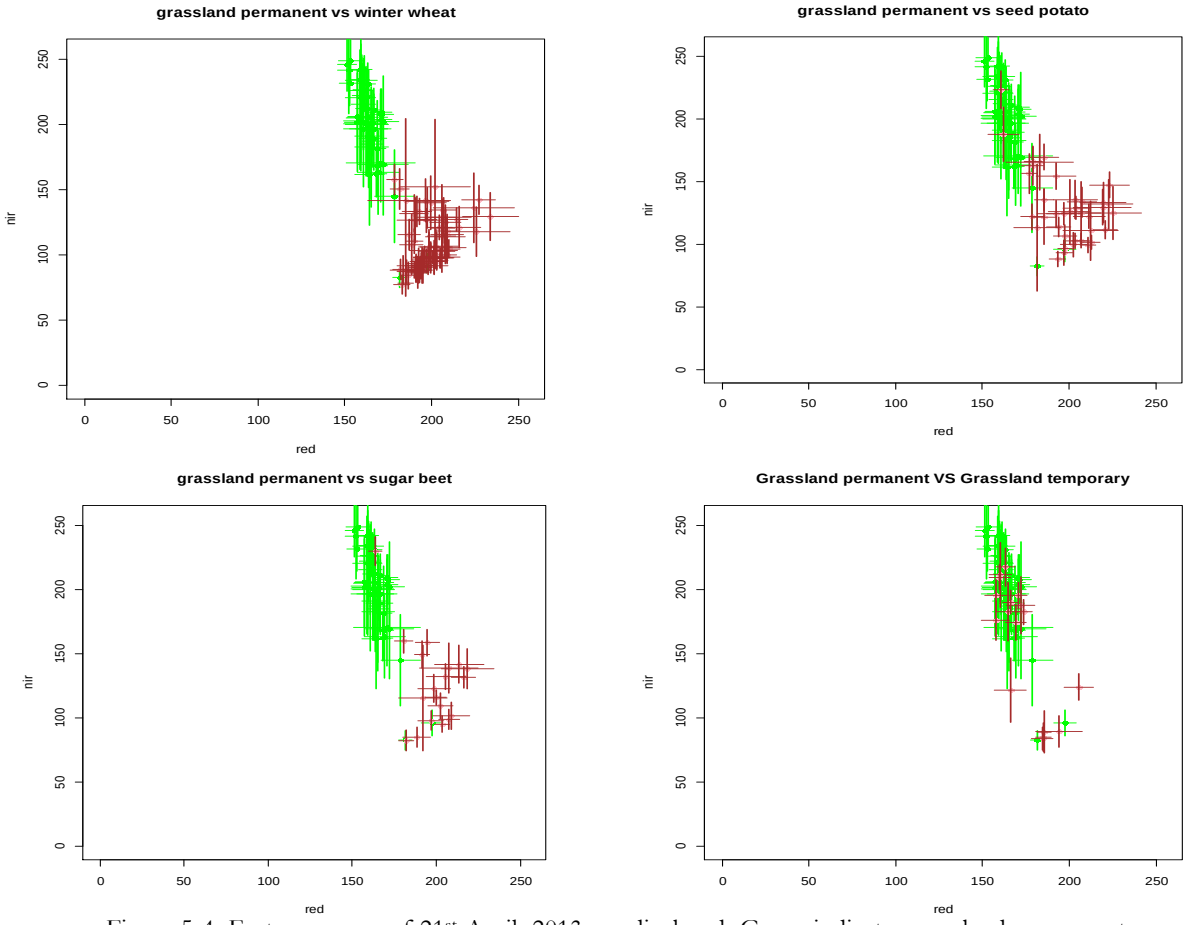

Figure 5-4: Feature spaces of 21st April, 2013 are displayed. Green indicates grassland permanent parcels with their standard deviations represented by lines. Brown indicates winter wheat in top left, seed potato in top right, sugar beet in bottom left and in bottom right grassland temporary.

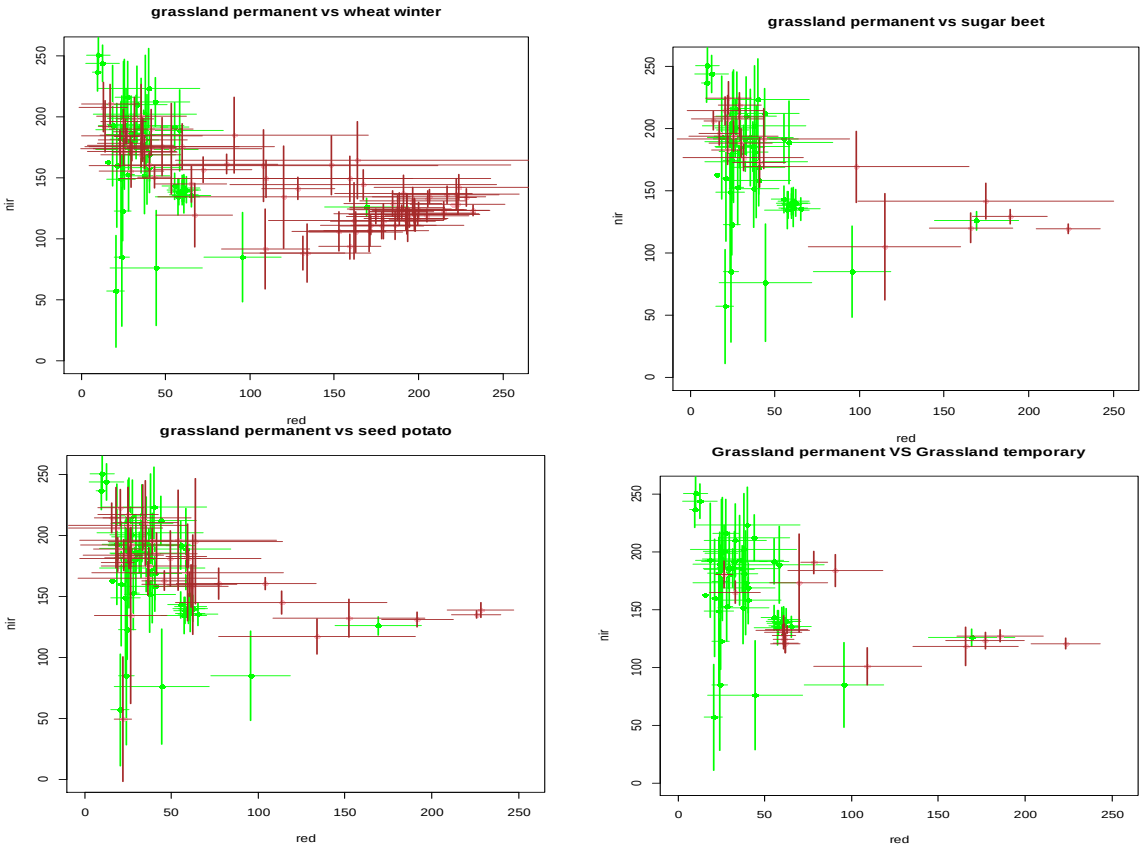

Figure 5-5: Feature spaces of 2nd June, 2013 are displayed. Green indicates grassland permanent parcels with their standard deviations represented by lines. Brown indicates winter wheat in top left, sugar beet in top right, seed potato in bottom left and grassland temporary in bottom right.

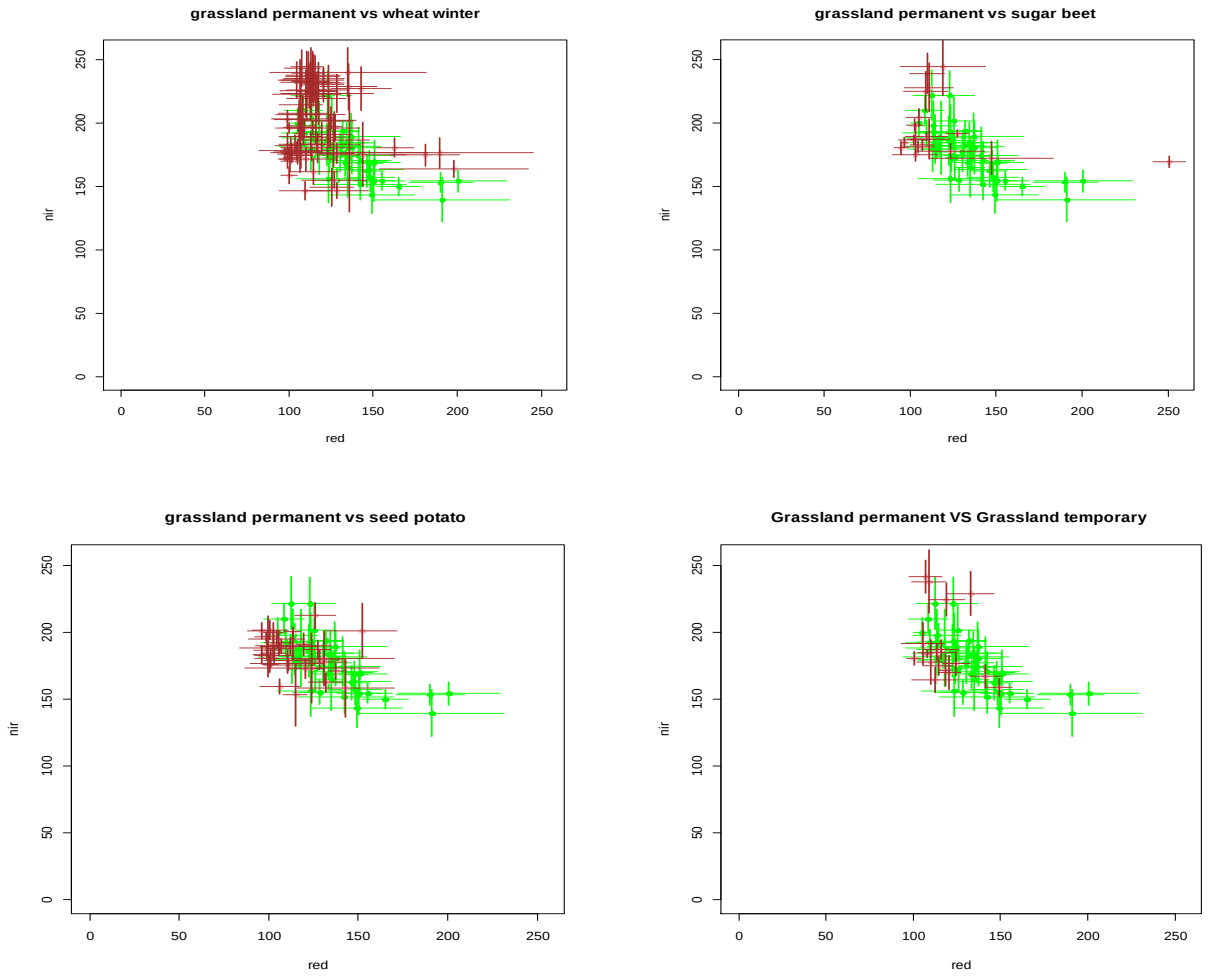

Figure 5-6: Feature spaces of 19th July, 2013 are displayed. Green indicates grassland permanent parcels with their standard deviations represented by lines. Brown indicates winter wheat in top left, sugar beet in top right, seed potato in bottom left and grassland temporary in bottom right.

5.3. Rule based classification

As discussed in the methodology section, the rules were made based on the feature space of different parcels. First classification technique applied was the single source analysis and then a combined analysis was performed on the results of single source analysis. The following sections would display the results in both the phases of classification and also discussion on the formulation of each rule to be used in the analysis.

5.3.1. First phase of classification

Starting with the 27th March, 2013 image, the rules defined for the following image used "if condition then inference" logical expression. The classes the image was defined are mixed parcel, bare land, uniform sparse vegetation, non-uniform sparse vegetation, uniform normal vegetation, non-uniform normal

vegetation and dense vegetation. The Figure 5-7 shows the classified map of 27th March, 2013 image with the classes discussed above.

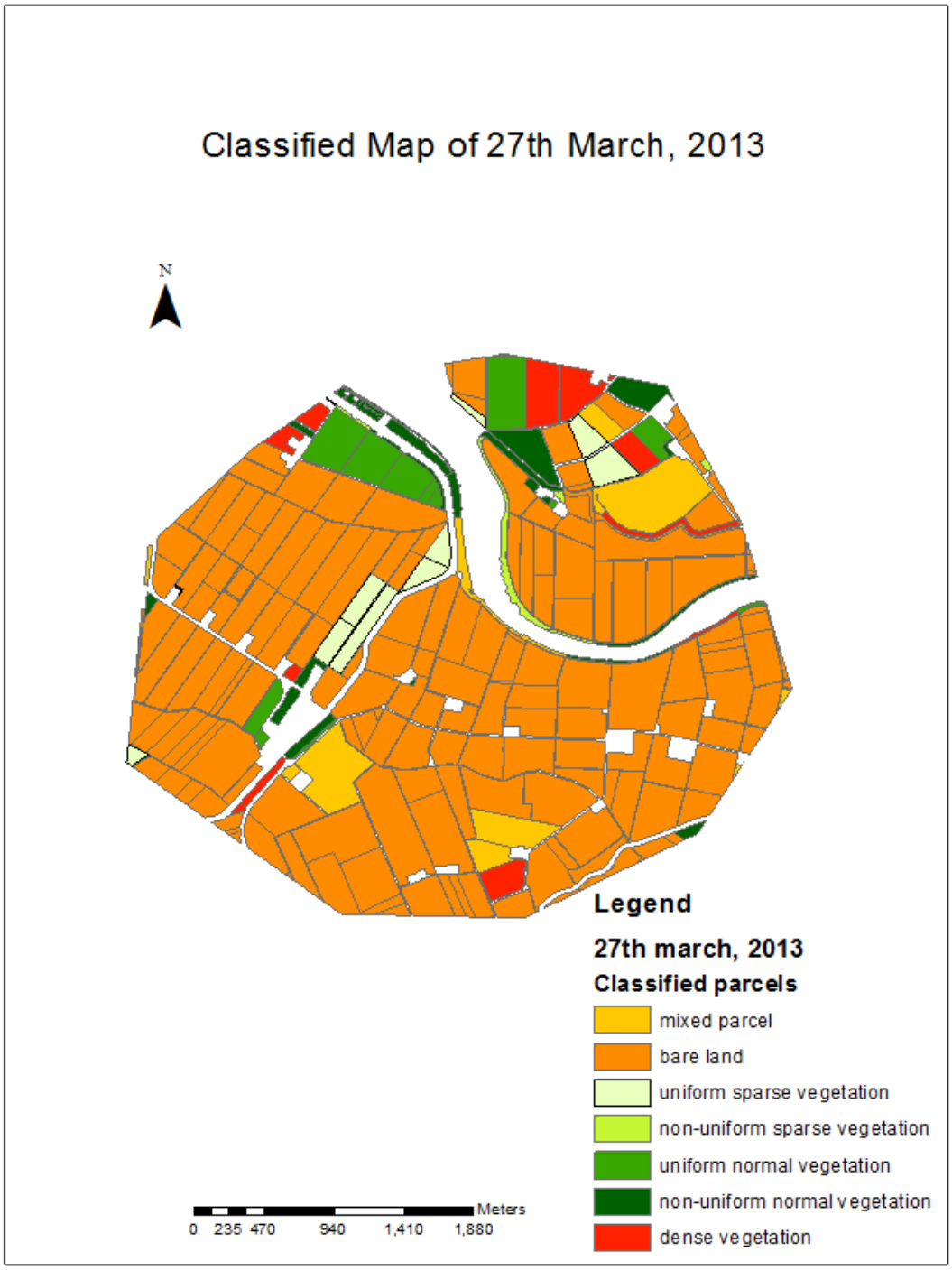

Figure 5-7: Classified map of 27th March, 2013 SPOT 5 image after the first phase of classification.

In the 21st April image the same process was applied as discussed in the 27th March image for producing a classified map but a new set of rules were defined based on parcel characteristics. The classes defined for the 21st April image are mixed parcel, bare land, very mild vegetation, uniform sparse vegetation, non-uniform sparse vegetation, uniform normal vegetation, non-uniform normal vegetation, dense vegetation.

A new class has been added here that is the very mild vegetation as there were some parcels where a slight growth of vegetation is spotted and image being a very high resolution image could spot such change. The rules for classifying this image are:

The classified map of 21st April is shown in Figure 5-8.

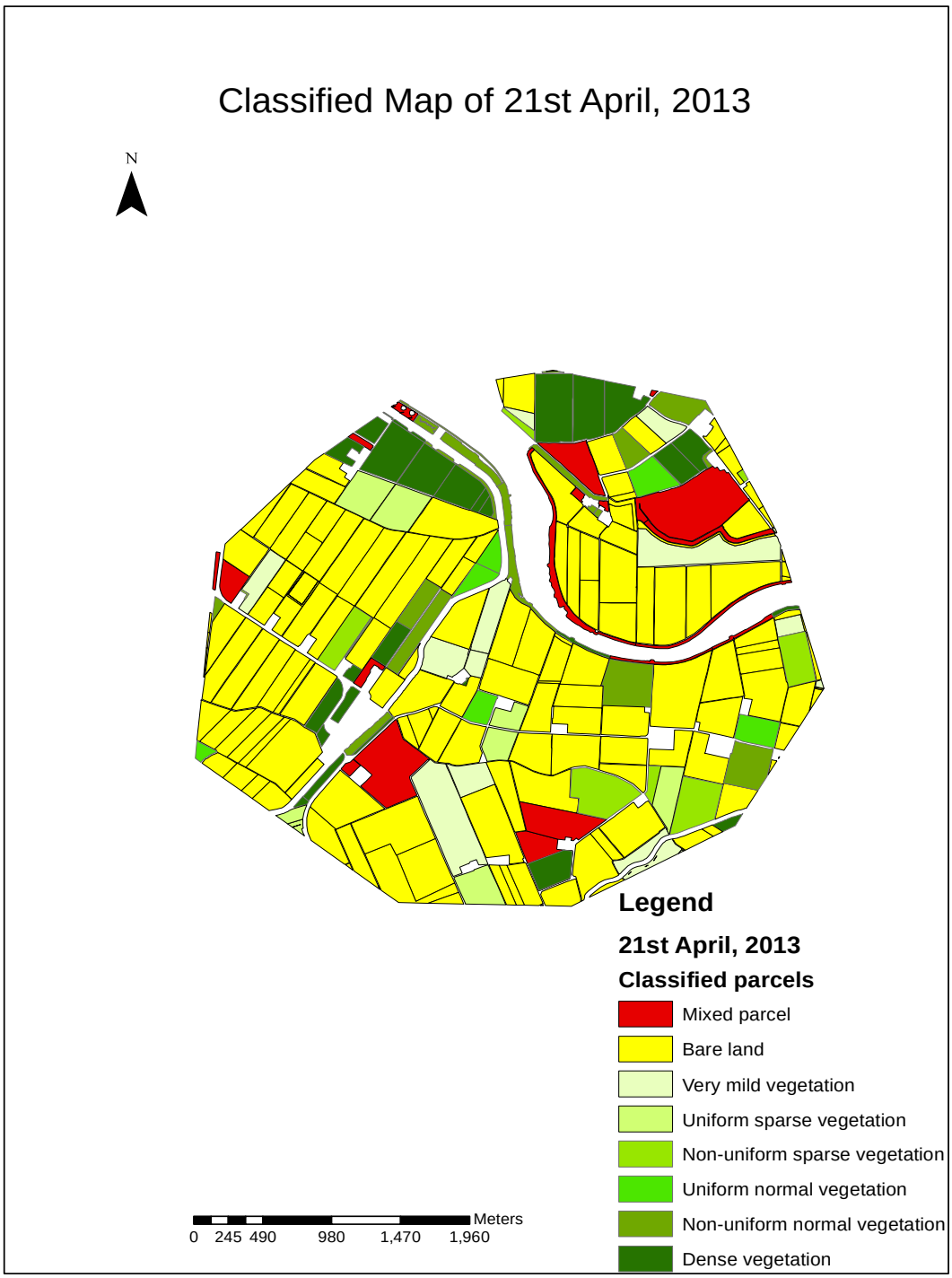

Figure 5-8: Classified map of 21st April, 2013 image after the first phase of classification.

Moving on to the 2nd June, 2013 image, similar analysis has been performed on it as discussed in the earlier images. The uniform and non-uniform parcel clause which defines the evenness of pixels in the parcels

has not been included in the rules formation as in the feature space most of the parcels had high standard deviations in both near infra-red and red bands. The classes defined for the image are mixed parcel, bare land, sparse vegetation, normal vegetation, dense vegetation.

The classified map of 2nd June is shown in Figure 5-9.

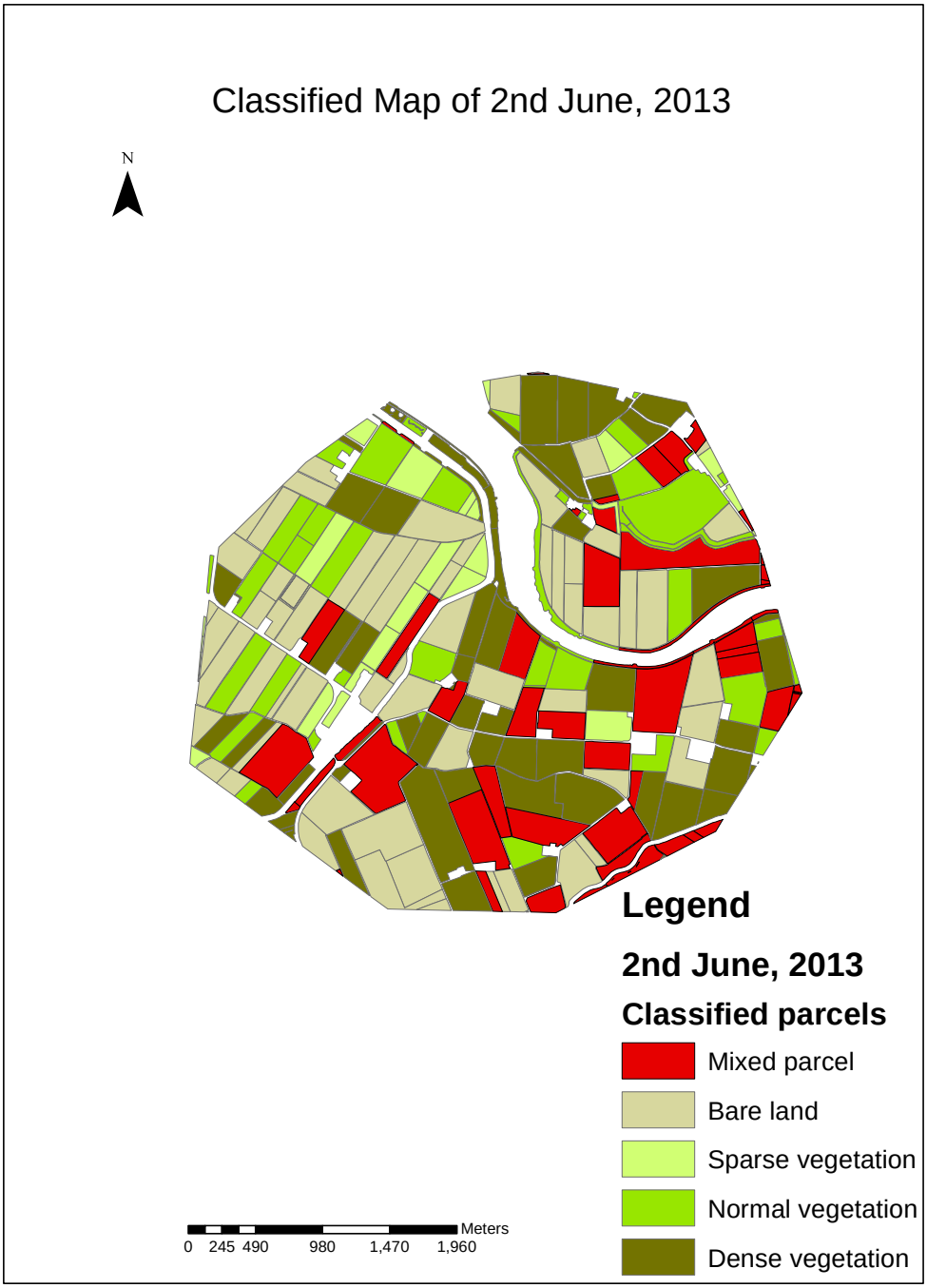

Figure 5-9: Classified map of 2nd June, 2013 SPOT 6 image after the first phase of classification.

The 19th July, 2013 image is also classified using the same approach discussed for the classification of previous images. The classes defined for the present image are mixed parcel, bare land, uniform sparse vegetation, non-uniform sparse vegetation, uniform normal vegetation, non-uniform normal vegetation, uniform dense vegetation and non-uniform dense vegetation. The classified map is displayed in Figure 5-10.

F

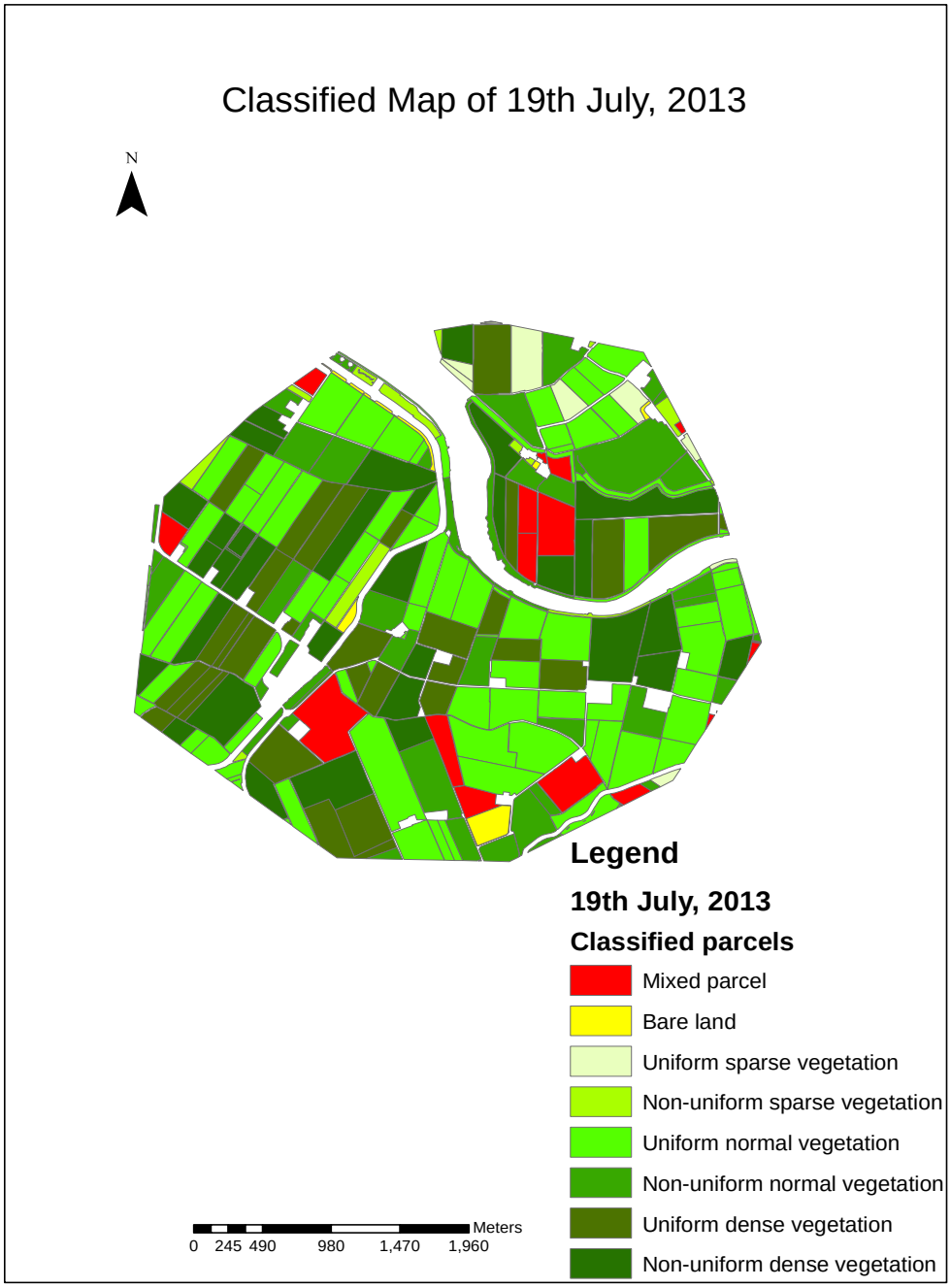

Figure 5-10: Classified map of 19th July, 2013 SPOT 5 after first phase of classification.

5.3.2. Final phase of classification

In the final phase of classification, as discussed in the methodology section, it uses the results obtained in the first phase of classification as its basic classification criteria. By taking some sample parcels of a

particular type of parcel, the classes of these sample parcels would be used for further classifying the desired parcel type.

For the process of classification, half the parcels of a particular type were taken for the classification and the rest were used for the validation of the parcel type. The major classification classes formed were mixed parcel, temporary grassland, permanent grassland, winter wheat, sugar beet, seed potato and consumption potato. There were total of 14 types of parcels in the reference data but only those parcels types have been taken whose parcels are more than three.

The final classified result is shown in Figure 5-11.

Figure 5-11: Classified map of 2013 displaying different crop types with permanent and temporary grassland.

5.3.3. Accuracy assessment

The accuracy assessment was calculated using confusion matrix. The mixed parcel class formed in the second phase of classification was not included in the error matrix and also the number of parcels of this class is subtracted from the number of parcels of a particular class type of the reference data before calculating the accuracy. This is because the class mixed parcel formed during the first phase of classification is only used for forming the class of mixed parcel again in the final phase of classification and not for classifying other classes in the final phase classification. It was deliberately done as mixed parcel class could not provide any reason to be included for classifying classes in the final phase of classification.

The confusion matrix is shown in Table 5-1.

Table 5-1: Confusion matrix of the final classification result.

	Permanent Grassland	**Temporary Grassland**	**Winter wheat**	**Seed potatoes**	**Sugar beet**	**User Accuracy (%)**	**Overall accuracy (%)**
Permanent Grassland	6	0	2	0	0	75	38.23
Temporary Grassland	3	3	2	0	0	60	
Winter wheat	0	0	15	6	2	65.21	
Seed potatoes	0	0	2	2		50	
Sugar beet	0	0	2	0	0	0	
Unclassified parcels	2	1	0	0	0		
Producer Accuracy (%)	54.54	75	65.21	25	0		

Overall accuracy = 38.23%

6. DISCUSSION

The objective of this research was to use the multi-sensor data and classify crop types by using rule based and object based approach.

6.1. Data pre-processing

Pre-processing of the data has been crucial as the images were from different sensors. For this reason geometric transformation on 2nd June, 2013 Spot 6 image and radiometric calibration on all the images was applied. Geo-referencing of the 2nd June, 2013 image of Spot 6 was performed as it was necessary for all images to have the same geometric transformation as the vector data since parcel statistics was needed to be extracted, an RMSE error of less than 0.5 pixels was attained which is acceptable. Radiometric calibration was the other phenomena required for all the images to be in the same radiometric resolution as they can be comparable. For this reason a linear stretching method was applied which stretched the 16 bit radiometric resolution images into the range of 0-255 and also the 8 bit images were stretched to bring all the images of same radiometric resolution. The linear stretching of an image generally expands the original values into a new set of distribution, this helps in displaying the minute variations in an image. As the value of a pixel is changing while stretching, it would surely have an effect on the quantitative information derived from it. The stretching of 16bit to 8 bit is actually decreasing the range of brightness of a pixel but it is also decreasing the variation in brightness between different pixels and this would help in forming nearly same classes for images for the same radiometric resolutions. Gillespie et al. (1986) discussed that in a multispectral image, spectrally featureless scenes have high correlation between different bands and information is difficult to obtain but if these bands are stretched then it would expand the dark-light range of intensities. It also explains that in a poorly correlated data, digital number pairs are present away from the equal-intensity line, stretching would fill the intensity range without saturating much data on either end of the range (Gillespie et al., 1986).

6.2. Data analysis

The parcel statistics obtained from parcels had mean and standard deviation values for every band. The statistical information was then used for plotting it in the feature space. The feature space formed using the stretched near infra-red and red bands clearly displayed the spread of parcels of particular type and also the separation between different parcels types also increased. Vegetation indices were calculated from the stretched images for each parcel which was later used for classifying the images. Normalized differential vegetation index (NDVI) would surely vary if the range of values of near infra-red is pretty much same and red differs but since the range of red differs much there would be a change in NDVI for different parcel types. The feature space was used here primarily for forming different rules for forming classes. By using feature space it becomes easier to identify outliers and clusters so that based on them rules can be defined. Displaying the standard deviations in feature space would help in identifying mixed

parcels if their standard deviation is large compared to the standard deviation of other parcels. Through standard deviation one can understand that the stages of growth of crops in a parcel, this also suggests if there is a high or low variation in the crop parcels.

6.3. Rule based classification

Rule based classification can be an effective tool for classification as it can handle multi sensor data effectively. Different images can have different set of rules for the classification, so for this reason rule based classification was adopted for the present research. Another advantage of using rule based classification is that the result can always be improved by using different datasets (Richards, 2013a). Rules can easily be updated altogether and be used again for a new set of images. The disadvantage in using them is that rules need to be formulated manually which is a laborious work where as these days in a computer driven world results are expected to be delivered fast and the method need to be robust. One of the disadvantage of using rule based systems are the high computational time, for small area it is taking lot of time then there would be serious problems if large areas and more datasets are considered. A two phased joint analysis was carried out in this research, being very detailed since every image would have its own rule base which can be updated anytime, and it is proved unnecessary in the end. Data storage is increased with different rule base for different images, a single rule base for the whole classification can be easier to store as it would have lesser rules for the classification.

In the first phase of classification, images were classified into different classification classes like mixed parcel, bare land, and uniform & non-uniform vegetation type based on standard deviation for sparse, normal and dense vegetation. The main purpose for such a basic classification was to relate the classified parcels with the principal growth stage of crops proposed by Meier (1997). But classes could not be similar as different sensor images have different spectral reflectance and spatial resolutions. Similar classes would have been easier to deduce as they can be easily compared and with this classes could be easily separated.

The use of normalized differential vegetation index (NDVI) and standard deviation were instrumental in classifying these images. The NDVI values which are taken from stretched images would vary in results if used for un-stretched images, so these can be used only for images from the same sensor and those which are stretched.

Final phase of classification uses the reference data with the previous classified results to form different parcel type classes. Half the reference data of a particular parcel type is used for training and the other half for validation. Crop types which are having less than 10 parcels have been left as they do not have many parcels to train and validate. The first class which was formed was mixed parcel. Mixed parcel as a class had a very significant place as these are those parcels which have been mixed parcels in all the images. Mixed parcel as a class from the first phase of classification cannot be an element in the final phase of classification as it does not represent a specific character of a parcel but it can keep a record on the parcels having different crop types for the subsidy allocation program. All the other class types in the final phase of classification are classified based on the most distinct type of the parcel for a particular date and

majority characteristic of that parcel. It was very tough separating different crop types as they would share same majority characteristic for a particular parcel type. Classification for classifying different parcel type could also be performed in the first step of classification but since most of the crop types were concentrated in clusters in 27th March image and 19th July image which makes it difficult to classify them.

The mixed parcels were removed for the accuracy assessment and so only those parcels which are not mixed parcel are classified. The segmentation of the mixed parcel and further dividing it into different parcels would have been beneficial.

The overall accuracy was 38.23% (Table 5-1). Accuracy is also highly influenced by the acquisition dates of the images, as better the dates to distinguish parcel types the better would be the classification result (Peña-Barragán et al., 2011). The 19th July, 2013 SPOT 5 image was highly confusing as all the crop parcels were highly vegetated at that time. An image of a later date near to September could have proved better as many crops are harvested at that time, so that would have made it easier to classify and get better accuracy. Only five classes have classified here so taking of more five classes would not have intelligent as it would much decrease the accuracy. One of the other reasons for such low accuracy was the logic used in the final classification phase regarding majority characteristic of class for a particular parcel. An expert knowledge about the growth of crops and harvesting of a particular region is always be helpful in improving the classification results. The other reason for low accuracy can be the reference data which was prepared by the farmers in 2012 about what they were planning to grow in 2013, so there is an uncertainty factor involved in the dataset as it is not a ground truth information but rather a pre-decided notion based on which the present research is dealt with.

7. CONCLUSIONS AND RECOMMENDATIONS

The main objective of this research is to use the multi-sensor images and classify crop types using object oriented and rule based approach.

The following sub-objectives which are completed are the following:

- To pre-process multi-sensor images through radiometric calibration.
- To get per parcel statistical information of each image by overlaying vector polygon data.
- To generate feature spaces of crop parcels and study them by comparing different crop types.
- To form rules for each sensor image based on the analysis of feature spaces of different crops and the temporal change in crop parcels.
- To check the accuracy of the classified map using ground truth data.

The linear stretching of all images for radiometric calibration was needed before the classification was performed as it would bring all images into same radiometric resolution which would make them easily comparable in defining rules. The use of joint rule based analysis was performed focussing on the need to study the texture and composition of a parcel at specific time so that these classified results from the first phase can be used to define rules for the final phase of classification. The present classification result was unsatisfactory as the accuracy was low. There were many cases discussed regarding the accuracy out of which if the time of data to be collected is kept in mind there would have been improvement in the accuracy. Other than this the method adopted in the final phase classification of majority characteristic did not work well as many crop types were showing same characteristic which made it difficult to separate them. Tackling multi sensor images individually and forming rules is not that satisfactory but a single rule base for a group of sensor images can be more innovative and much productive. Overall the use of multi sensor images has a bright path in the present world where satellite missions have increased tremendously.

The research questions that were raised for the formulation for these objectives are answered in the following section.

7.1. Conclusion

The research questions make the conclusion by adding answers to it.

- How to handle differences in radiometric resolution in multi sensor images?

The radiometric resolution of all the images can be brought to the same resolution through "Linear contrast stretching".

- Does the combined use of multi-sensor images can provide better results in crop identification than single sensor images?

Single sensor images have same resolution but for crop identification type of application single sensor images need to have high temporary resolution. In multi-sensor image, every image has different

radiometric and spatial resolutions. This information could provide much better classification result using multi-sensor data.

- How to define rules using feature space of parcels of different crop types and grassland?

First permanent grassland would be represented in the feature space. Outliers and pixels in the clusters will be analysed based on which basic classes will be formed and after which other crop types are also plotted in the feature space but against permanent grassland.

- Is the use of multiple-rule base approach better than single rule base in the present study of crop classification?

The use of multiple rule bases is better as separate rules can be made for each image and then finally classify using a joint rule base approach. The rules can be edited anytime and new datasets can also be added in the rule base.

- What would be the performance quality of this classification method in terms of speed and accuracy?

The accuracy is low but it is based on many factors discussed in the previous section. The speed of the classification is average. Overall the present classification technique is not feasible for classifying crop types as it produces low accuracy.

7.2. Recommendations

The textural features of the parcels could provide extra input about the texture of the parcel for a respective date. Recommendations for further research are summarised here:

- The use of pixel based information in combination with parcel based information can be interesting area of study.
- Single phase classification technique could be implemented and a single rule base should be constructed for multi sensor images.
- Use of expert knowledge can be an asset as it can improve the classification accuracy.

LIST OF REFERENCES

Amorós-López, J., Gómez-Chova, L., Alonso, L., Guanter, L., Zurita-Milla, R., Moreno, J., & Camps-Valls, G. (2013). Multitemporal fusion of Landsat/TM and ENVISAT/MERIS for crop monitoring. *International Journal of Applied Earth Observation and Geoinformation, 23*(0), 132-141. doi: http://dx.doi.org/10.1016/j.jag.2012.12.004

Bakx, J. P. G., Gorte, B. G. H., Feringa, W. F., Grabmaier, K. A., Janssen, L., Kerle, N., . . . Woldai, T. (2012). In V. A. T. a. A. Stein (Ed.), *The core of GIScience : a systems - based approach* (pp. 167-204). Enschede: University of Twente Faculty of Geo-Information and Earth Observation (ITC).

Baret, F., Guyot, G., & Major, D. (1989). *TSAVI: a vegetation index which minimizes soil brightness effects on LAI and APAR estimation.* Paper presented at the Geoscience and Remote Sensing Symposium, 1989. IGARSS'89. 12th Canadian Symposium on Remote Sensing., 1989 International.

Benz, U. C., Hofmann, P., Willhauck, G., Lingenfelder, I., & Heynen, M. (2004). Multi-resolution, object-oriented fuzzy analysis of remote sensing data for GIS-ready information. *ISPRS Journal of Photogrammetry and Remote Sensing, 58*(3), 239-258.

Blaschke, T. (2010). Object based image analysis for remote sensing. *ISPRS Journal of Photogrammetry and Remote Sensing, 65*(1), 2-16. doi: http://dx.doi.org/10.1016/j.isprsjprs.2009.06.004

Clark, B., Suomalainen, J., & Pellikka, P. (2011). An historical empirical line method for the retrieval of surface reflectance factor from multi-temporal SPOT HRV, HRVIR and HRG multispectral satellite imagery. *International Journal of Applied Earth Observation and Geoinformation, 13*(2), 292-307. doi: http://dx.doi.org/10.1016/j.jag.2010.12.004

Clevers, J. G. P. W. (1988). The derivation of a simplified reflectance model for the estimation of leaf area index. *Remote Sensing of Environment, 25*(1), 53-69. doi: http://dx.doi.org/10.1016/0034-4257(88)90041-7

Diaz-Varela, R. A., Zarco-Tejada, P. J., Angileri, V., & Loudjani, P. (2014). Automatic identification of agricultural terraces through object-oriented analysis of very high resolution DSMs and multispectral imagery obtained from an unmanned aerial vehicle. *Journal of Environmental Management, 134*(0), 117-126. doi: http://dx.doi.org/10.1016/j.jenvman.2014.01.006

Duro, D. C., Franklin, S. E., & Dubé, M. G. (2012). A comparison of pixel-based and object-based image analysis with selected machine learning algorithms for the classification of agricultural landscapes using SPOT-5 HRG imagery. *Remote Sensing of Environment, 118*(0), 259-272. doi: http://dx.doi.org/10.1016/j.rse.2011.11.020

Esch, T., Metz, A., Marconcini, M., & Keil, M. (2014). Combined use of multi-seasonal high and medium resolution satellite imagery for parcel-related mapping of cropland and grassland. *International Journal of Applied Earth Observation and Geoinformation, 28*(0), 230-237. doi: http://dx.doi.org/10.1016/j.jag.2013.12.007

European Commission. (11-02-2014). Agriculture and Rural Development. Retrieved 15-02-2014, from http://ec.europa.eu/agriculture/cap-history/index_en.htm

http://ec.europa.eu/agriculture/climate-change/index_en.htm

FAO. (2012, 07-02-2014). FAOSTAT. Retrieved 15-02-2014, 2014, from http://faostat.fao.org/site/567/DesktopDefault.aspx?PageID=567#ancor

Foerster, S., Kaden, K., Foerster, M., & Itzerott, S. (2012). Crop type mapping using spectral–temporal profiles and phenological information. *Computers and Electronics in Agriculture, 89*(0), 30-40. doi: http://dx.doi.org/10.1016/j.compag.2012.07.015

Foucher, S., Germain, M., Boucher, J. M., & Benie, G. B. (2002). Multisource classification using ICM and Dempster-Shafer theory. *Instrumentation and Measurement, IEEE Transactions on, 51*(2), 277-281. doi: 10.1109/19.997824

Gao, B.-c. (1996). NDWI—A normalized difference water index for remote sensing of vegetation liquid water from space. *Remote Sensing of Environment, 58*(3), 257-266. doi: http://dx.doi.org/10.1016/S0034-4257(96)00067-3

Geneletti, D., & Gorte, B. G. H. (2003). A method for object-oriented land cover classification combining Landsat TM data and aerial photographs. *International Journal of Remote Sensing, 24*(6), 1273-1286. doi: 10.1080/01431160210144499

Giakoumakis, M., Gitas, I., & San-Miguel, J. (2002). Object-oriented classification modelling for fuel type mapping in the Mediterranean, using LANDSAT TM and IKONOS imagery—preliminary results. *Forest Fires Research & Wildland Fire Safety. Millpress, Rotterdam*.

Gillespie, A. R., Kahle, A. B., & Walker, R. E. (1986). Color enhancement of highly correlated images. I. Decorrelation and HSI contrast stretches. *Remote Sensing of Environment, 20*(3), 209-235. doi: http://dx.doi.org/10.1016/0034-4257(86)90044-1

Government of Canada, N. R. C. (30-01-2014). Crop Type Mapping | Earth Sciences. from http://www.nrcan.gc.ca/earth-sciences/geomatics/satellite-imagery-air-photos/satellite-imagery-products/educational-resources/14649

Hall, F. G., Strebel, D. E., Nickeson, J. E., & Goetz, S. J. (1991). Radiometric rectification: Toward a common radiometric response among multidate, multisensor images. *Remote Sensing of Environment, 35*(1), 11-27. doi: http://dx.doi.org/10.1016/0034-4257(91)90062-B

Hardisky, M., Klemas, V., & Smart, M. (1983). The influence of soil salinity, growth form, and leaf moisture on the spectral radiance of. *Spartina alterniflora*, 77-83.

Huete, A. R. (1988). A soil-adjusted vegetation index (SAVI). *Remote Sensing of Environment, 25*(3), 295-309. doi: http://dx.doi.org/10.1016/0034-4257(88)90106-X

Huete, A. R., Jackson, R. D., & Post, D. F. (1985). Spectral response of a plant canopy with different soil backgrounds. *Remote Sensing of Environment, 17*(1), 37-53. doi: http://dx.doi.org/10.1016/0034-4257(85)90111-7

Jakubauskas, M. E., Legates, D. R., & Kastens, J. H. (2002). Crop identification using harmonic analysis of time-series AVHRR NDVI data. *Computers and Electronics in Agriculture, 37*(1–3), 127-139. doi: http://dx.doi.org/10.1016/S0168-1699(02)00116-3

Jiang, J., Li, A., Deng, W., & Bian, J. (2010). Construction of a New Classifier Integrated Multiple Sources and Multi-temporal Remote Sensing Data for wetlands. *Procedia Environmental Sciences, 2*(0), 302-314. doi: http://dx.doi.org/10.1016/j.proenv.2010.10.036

Jurgens, C. (1997). The modified normalized difference vegetation index (mNDVI) a new index to determine frost damages in agriculture based on Landsat TM data. *International Journal of Remote Sensing, 18*(17), 3583-3594. doi: 10.1080/014311697216810

Kowalik, W. S., Marsh, S. E., & Lyon, R. J. P. (1982). A relation between landsat digital numbers, surface reflectance, and the cosine of the solar zenith angle. *Remote Sensing of Environment, 12*(1), 39-55. doi: http://dx.doi.org/10.1016/0034-4257(82)90006-2

Kurukulasuriya, P., & Rosenthal, S. (2003). Climate Change and Agriculture.

Laliberte, A. S., Rango, A., Havstad, K. M., Paris, J. F., Beck, R. F., McNeely, R., & Gonzalez, A. L. (2004). Object-oriented image analysis for mapping shrub encroachment from 1937 to 2003 in southern New Mexico. *Remote Sensing of Environment, 93*(1–2), 198-210. doi: http://dx.doi.org/10.1016/j.rse.2004.07.011

Liu, Y., Li, M., Mao, L., Xu, F., & Huang, S. (2006). Review of remotely sensed imagery classification patterns based on object-oriented image analysis. *Chinese Geographical Science, 16*(3), 282-288. doi: 10.1007/s11769-006-0282-0

Löw, F., Michel, U., Dech, S., & Conrad, C. (2013). Impact of feature selection on the accuracy and spatial uncertainty of per-field crop classification using Support Vector Machines. *ISPRS Journal of Photogrammetry and Remote Sensing, 85*(0), 102-119. doi: http://dx.doi.org/10.1016/j.isprsjprs.2013.08.007

Lucas, R., Rowlands, A., Brown, A., Keyworth, S., & Bunting, P. (2007). Rule-based classification of multi-temporal satellite imagery for habitat and agricultural land cover mapping. *ISPRS Journal of Photogrammetry and Remote Sensing, 62*(3), 165-185. doi: http://dx.doi.org/10.1016/j.isprsjprs.2007.03.003

Martínez-Casasnovas, J. A., Martín-Montero, A., & Auxiliadora Casterad, M. (2005). Mapping multi-year cropping patterns in small irrigation districts from time-series analysis of Landsat TM images. *European Journal of Agronomy, 23*(2), 159-169. doi: http://dx.doi.org/10.1016/j.eja.2004.11.004

Masek, J. G., Vermote, E. F., Saleous, N. E., Wolfe, R., Hall, F. G., Huemmrich, K. F., . . . Teng-Kui, L. (2006). A Landsat surface reflectance dataset for North America, 1990-2000. *Geoscience and Remote Sensing Letters, IEEE, 3*(1), 68-72. doi: 10.1109/LGRS.2005.857030

Meier, U. B. B. f. L.-u. F. (1997). *Growth stages of mono- and dicotyledonous plants : BBCH-Monograph*. Berlin; Boston: Blackwell Wissenschafts-Verlag.

Melgani, F., & Serpico, S. B. (2002). A statistical approach to the fusion of spectral and spatio-temporal contextual information for the classification of remote-sensing images. *Pattern Recognition Letters, 23*(9), 1053-1061. doi: http://dx.doi.org/10.1016/S0167-8655(02)00052-1

Moran, M. S., Bryant, R., Thome, K., Ni, W., Nouvellon, Y., Gonzalez-Dugo, M. P., . . . Clarke, T. R. (2001). A refined empirical line approach for reflectance factor retrieval from Landsat-5 TM and Landsat-7 ETM+. *Remote Sensing of Environment, 78*(1–2), 71-82. doi: http://dx.doi.org/10.1016/S0034-4257(01)00250-4

Moran, M. S., Jackson, R. D., Clarke, T. R., Qi, J., Cabot, F., Thome, K. J., & Markha, B. L. (1995). Reflectance factor retrieval from Landsat TM and SPOT HRV data for bright and dark targets. *Remote Sensing of Environment, 52*(3), 218-230. doi: http://dx.doi.org/10.1016/0034-4257(95)00035-Y

Ozdogan, M. (2010). The spatial distribution of crop types from MODIS data: Temporal unmixing using Independent Component Analysis. *Remote Sensing of Environment, 114*(6), 1190-1204. doi: http://dx.doi.org/10.1016/j.rse.2010.01.006

Panigrahy, S., & Sharma, S. A. (1997). Mapping of crop rotation using multidate Indian Remote Sensing Satellite digital data. *ISPRS Journal of Photogrammetry and Remote Sensing, 52*(2), 85-91. doi: http://dx.doi.org/10.1016/S0924-2716(97)83003-1

Pearson, R. L., & Miller, L. D. (1972). {*Remote mapping of standing crop biomass for estimation of the productivity of the short-grass Prairie, Pawnee National Grasslands, Colorado*}. Paper presented at the Proceedings of the Eighth International Symposium on Remote Sensing of Environment.

Peña-Barragán, J. M., Ngugi, M. K., Plant, R. E., & Six, J. (2011). Object-based crop identification using multiple vegetation indices, textural features and crop phenology. *Remote Sensing of Environment, 115*(6), 1301-1316. doi: http://dx.doi.org/10.1016/j.rse.2011.01.009

Petitjean, F., Inglada, J., & Gançarski, P. (2012). Satellite image time series analysis under time warping. *Geoscience and Remote Sensing, IEEE Transactions on, 50*(8), 3081-3095.

Qi, J., Chehbouni, A., Huete, A. R., Kerr, Y. H., & Sorooshian, S. (1994). A modified soil adjusted vegetation index. *Remote Sensing of Environment, 48*(2), 119-126. doi: http://dx.doi.org/10.1016/0034-4257(94)90134-1

Qi, J., Kerr, Y., & Chehbouni, A. (1994). External factor consideration in vegetation index development.

Reichert, T. (2006). A Closer Look at EU Agricultural Subsidies. http://germanwatch.org/tw/eu-agr05e.pdf

Richards, J. (2013a). Multisource Image Analysis *Remote Sensing Digital Image Analysis* (pp. 437-464): Springer Berlin Heidelberg.

Richards, J. (2013b). Spectral Domain Image Transforms *Remote Sensing Digital Image Analysis* (pp. 161-201): Springer Berlin Heidelberg.

Rouse, J. W., Haas, R. H., & Schell, J. A. (1974). *Monitoring the vernal advancement and retrogradation (greenwave effect) of natural vegetation*. College Station: Texas A and M University.

Schowengerdt, R. A. (2007). Chapter 1 - The nature of remote sensing. In R. A. Schowengerdt (Ed.), *Remote Sensing (Third edition)* (pp. 1-X). Burlington: Academic Press.

Smith, G. M., & Milton, E. J. (1999). The use of the empirical line method to calibrate remotely sensed data to reflectance. *International Journal of Remote Sensing, 20*(13), 2653-2662. doi: 10.1080/014311699211994

Solberg, A. H. S., Taxt, T., & Jain, A. K. (1996). A Markov random field model for classification of multisource satellite imagery. *Geoscience and Remote Sensing, IEEE Transactions on, 34*(1), 100-113. doi: 10.1109/36.481897

Tucker, C. J. (1980). Remote sensing of leaf water content in the near infrared. *Remote Sensing of Environment, 10*(1), 23-32. doi: http://dx.doi.org/10.1016/0034-4257(80)90096-6

Ünsalan, C., & Boyer, K. (2011). Linearized Vegetation Indices *Multispectral Satellite Image Understanding* (pp. 19-39): Springer London.

Van Niel, T. G., & McVicar, T. R. (2004). Determining temporal windows for crop discrimination with remote sensing: a case study in south-eastern Australia. *Computers and Electronics in Agriculture, 45*(1–3), 91-108. doi: http://dx.doi.org/10.1016/j.compag.2004.06.003

Waldhoff, G., & Bareth, G. (2009). *GIS- and RS-based land use and land cover analysis: case study Rur-Watershed, Germany*.

Wu, Q., Li, H.-q., Wang, R.-s., Paulussen, J., He, Y., Wang, M., . . . Wang, Z. (2006). Monitoring and predicting land use change in Beijing using remote sensing and GIS. *Landscape and Urban Planning, 78*(4), 322-333. doi: http://dx.doi.org/10.1016/j.landurbplan.2005.10.002

Zhang, X., Friedl, M. A., Schaaf, C. B., Strahler, A. H., Hodges, J. C. F., Gao, F., . . . Huete, A. (2003). Monitoring vegetation phenology using MODIS. *Remote Sensing of Environment, 84*(3), 471-475. doi: http://dx.doi.org/10.1016/S0034-4257(02)00135-9

Zhang, X., Sun, R., Zhang, B., & Tong, Q. (2008). Land cover classification of the North China Plain using MODIS_EVI time series. *ISPRS Journal of Photogrammetry and Remote Sensing, 63*(4), 476-484. doi: http://dx.doi.org/10.1016/j.isprsjprs.2008.02.005

Zhou, W., & Troy, A. (2008). An object-oriented approach for analysing and characterizing urban landscape at the parcel level. *International Journal of Remote Sensing, 29*(11), 3119-3135.

APPENDIX (A)

1. R CODE (Linear stretching)

```
rm(list=ls(all=TRUE))
require(rgdal)
require(rgl)
require(maptools)

StartPath <- getwd()

#Defining the root directory
Root <- "E:/Programming/Emani"

Path_in <- paste(Root, "/Input",sep="")
Path_out <- paste(Root, "/Output",sep="")

dir.create(Path_out,showWarnings=FALSE, recursive=TRUE)

hist.strecth <- function(x)
{
    n <- dim(x)[2]
    for(k in 1:n)
    {
        data <- x[,k]
        cur.lim <- quantile(data,c(0.025,0.975),na.rm=TRUE)
        data <- pmax(cur.lim[1],pmin(cur.lim[2],data))
        data <- floor(255*(data-cur.lim[1])/(cur.lim[2]-cur.lim[1]))
        data[is.na(data)]<-0
        x[,k] <- data
    }
    return(x)
}
#============================================================================
============
# Read image
#============================================================================
============
image.fn <- "LAUW_20130327"

A <- readGDAL(paste(Path_in,"/",image.fn,".tif",sep=""))

Nb <- dim(A@data)[2]

#summary(A@data)

# Read vector file, for subsetting

vector.fn <- "extent"

V <- readOGR(paste(Path_in,"/",vector.fn, sep=""), layer=vector.fn)

i<-1
j<-1

polxy <- coordinates(V@polygons[[i]]@Polygons[[j]])

xy <- coordinates(A)

tmp <- point.in.polygon(xy[,1],xy[,2],polxy[,1],polxy[,2])
```

```
ind <- which(tmp==1)
indout<- which(tmp!=1)



minDN <- array(0,Nb)
maxDN <- array(0,Nb)

for(k in 1:Nb)
{
    x <- A@data[ind,]
    minDN[k] <- min(x[,k])
    data <- x[,k]
    maxDN[k] <- quantile(data,0.99,na.rm=TRUE)
}

Acalibrated <- A

for(k in 1:Nb)
{
    x <- A@data[ind,k]
    x <- x-minDN[k]
    x <- x*255/(maxDN[k]-minDN[k])

    x[x<0] <- 0
    x[x>255]<-255

    Acalibrated@data[ind,k] <- x
}


Acalibrated@data[indout,] <- 0
hist(Acalibrated@data$band4)

# output MRF solution to a .tif file
OUT <- Acalibrated
setwd(Path_out)

imagefn.out <- paste(image.fn,"_calibrated.tif",sep="")

OUT.tif<-create2GDAL(OUT,drivername="GTiff",type="Float32",mvFlag=-1)

saveDataset(OUT.tif,imagefn.out)
GDAL.close(OUT.tif)



setwd(StartPath)

# The End
```

2. RCODE (Training the parcels and extracting information)

```
rm(list=ls(all=TRUE))
require(rgdal)
require(rgl)
require(maptools)
require(raster)
```

```
StartPath <- getwd()

#Defining the root directory
Root <- "E:/Programming/Emani"

Path_in <- paste(Root, "/Input",sep="")
Path_out <- paste(Root, "/Output",sep="")

dir.create(Path_out,showWarnings=FALSE, recursive=TRUE)

hist.strecth <- function(x)
{
    n <- dim(x)[2]
    for(k in 1:n)
    {
        data <- x[,k]
        cur.lim <- quantile(data,c(0.025,0.975),na.rm=TRUE)
        data <- pmax(cur.lim[1],pmin(cur.lim[2],data))
        data <- floor(255*(data-cur.lim[1])/(cur.lim[2]-cur.lim[1]))
        data[is.na(data)]<-0
        x[,k] <- data
    }
    return(x)
}

Nim <- 4

Nb <- 4

mu <- array(0,c(Nim,Nb))
Cov <- array(0,c(Nim,Nb,Nb))
#============================================================================
============
# Read images
#============================================================================
============
im.names <-
c("27_march_calibrated","parcelDgrassland_temporary_calibrated","june2_fina
l2_calibrated","19_july_calibrated")
vector.fn <- "all_parcels"

# Read vector file, for subsetting
V <- readOGR(paste(Path_in,"/parcel_shapefiles/vectoe_extent", sep=""),
layer=vector.fn)
n.pol <- length(V)

V$class_id <- array(0,n.pol)

m <-4

image.fn <- im.names[m]

A <- readGDAL(paste(Path_in,"/",image.fn,".tif",sep=""))

Nb <- dim(A@data)[2]

xy <- coordinates(A)

image(A,red=1,green=2,blue=3,axes=TRUE)
```

```
hist(A@data$band4)

pol_col_arr <- c("green","yellow","brown")

pol_summary<-data.frame(array(NA,c(n.pol,12)))
names(pol_summary)<-
c("class_id","mu1","mu2","mu3","mu4","sd1","sd2","sd3","sd4","vi","ndvi","s
avi")

pol_summary[,1] <- as.numeric(unlist(V@data$GWS_GEWAS))

for(i in 1:n.pol)
{
    j<-1

    polxy <- coordinates(V@polygons[[i]]@Polygons[[j]])

    tmp <- point.in.polygon(xy[,1],xy[,2],polxy[,1],polxy[,2])
    ind <- which(tmp==1)

    if(length(ind)>0)
    {
        y <- A@data[ind,]
        mu[m,] <- colMeans(y, na.rm = TRUE)
        Cov[m,,] <- var(y, na.rm = TRUE)
        vi   <- (mu[m,1]/mu[m,2])
        ndvi <- ((mu[m,1]-mu[m,2])/(mu[m,1]+mu[m,2]))
        savi <- (((mu[m,1]-mu[m,2])/((mu[m,1]+mu[m,2])+(1/2)))*(3/2))
        pol_summary[i,2:5]<-mu[m,]
        pol_summary[i,6:9]<-sqrt(diag(Cov[m,,]))
        pol_summary[i,10]<-vi
        pol_summary[i,11]<-ndvi
        pol_summary[i,12]<-savi
    }
}

# Export results
write.table(pol_summary,paste(Path_out,"/training_summary_image_",m,".txt",
sep=""),row.names = FALSE)

# All classes

k <- 1
ind <- which(pol_summary$class_id==k)

plot(pol_summary$mu2[ind],pol_summary$mu1[ind],xlim=c(0,255),ylim=c(0,255),
pch=k,col=k,xlab="red",ylab="nir",main="")
title(main= "plot of all parcels_un_stretched")
for(k in 7:nlevels(V@data$GWS_GEWAS))
{
    ind <- which(pol_summary$class_id==k)
    points(pol_summary$mu2[ind],pol_summary$mu1[ind],pch=k,col=k)
}


# Only two classes (Feature space)


k <- 7
```

```
ind <- which(pol_summary$class_id==k)

plot(pol_summary$mu2[ind],pol_summary$mu1[ind],xlim=c(0,255),ylim=c(0,255),
pch=16,col="green",xlab="red",ylab="nir",main="")
#hist(pol_summary$mu2[ind])
title(main="Grassland permanent VS Grassland temporary ")
for(i in ind)
{
    lines(c(pol_summary$mu2[i],pol_summary$mu2[i]),c(pol_summary$mu1[i]-
pol_summary$sd1[i],pol_summary$mu1[i]+pol_summary$sd1[i]),col="green",lwd=2
)
    lines(c(pol_summary$mu2[i]-
pol_summary$sd2[i],pol_summary$mu2[i]+pol_summary$sd2[i]),c(pol_summary$mu1
[i],pol_summary$mu1[i]),col="green")
}


l <- 8
ind <- which(pol_summary$class_id==l)

points(pol_summary$mu2[ind],pol_summary$mu1[ind],pch=16,col="pink")

for(i in ind)
{
    lines(c(pol_summary$mu2[i],pol_summary$mu2[i]),c(pol_summary$mu1[i]-
pol_summary$sd1[i],pol_summary$mu1[i]+pol_summary$sd1[i]),col="brown",lwd=2
)
    lines(c(pol_summary$mu2[i]-
pol_summary$sd2[i],pol_summary$mu2[i]+pol_summary$sd2[i]),c(pol_summary$mu1
[i],pol_summary$mu1[i]),col="brown")
}
```

3. RCODE (Classification)

```
rm(list=ls(all=TRUE))
require(rgdal)
require(rgl)
require(maptools)
require(raster)

StartPath <- getwd()

#Defining the root directory
Root <- "E:/Programming/Emani"

Path_in <- paste(Root, "/Input",sep="")
Path_out <- paste(Root, "/Output",sep="")

dir.create(Path_out,showWarnings=FALSE, recursive=TRUE)

hist.strecth <- function(x)
{
    n <- dim(x)[2]
    for(k in 1:n)
    {
        data <- x[,k]
        cur.lim <- quantile(data,c(0.025,0.975),na.rm=TRUE)
        data <- pmax(cur.lim[1],pmin(cur.lim[2],data))
        data <- floor(255*(data-cur.lim[1])/(cur.lim[2]-cur.lim[1]))
```

```
        data[is.na(data)]<-0
        x[,k] <- data
    }
    return(x)
}

Nim <- 4

Nb <- 4

mu <- array(0,c(Nim,Nb))
Cov <- array(0,c(Nim,Nb,Nb))

#============================================================================
============
# Read images
#============================================================================
============
im.names <-
c("27_march_calibrated","parcelDgrassland_temporary_calibrated","june2_fina
l2_calibrated","19_july_calibrated")
vector.fn <- "all_parcels"

# Read vector file, for subsetting
V <- readOGR(paste(Path_in,"/parcel_shapefiles/vectoe_extent", sep=""),
layer=vector.fn)
n.pol <- length(V)



V$class_id <- array(0,n.pol)

m <-1

image.fn <- im.names[m]

A <- readGDAL(paste(Path_in,"/",image.fn,".tif",sep=""))

Nb <- dim(A@data)[2]

xy <- coordinates(A)

image(A,red=1,green=2,blue=3,axes=TRUE)

pol_col_arr <- c("red","yellow","pink","white","green","cyan","black")

for(i in 1:n.pol)
{
    j<-1

    polxy <- coordinates(V@polygons[[i]]@Polygons[[j]])

    tmp <- point.in.polygon(xy[,1],xy[,2],polxy[,1],polxy[,2])
    ind <- which(tmp==1)

    if(length(ind)>0)
    {
        y <- A@data[ind,]
        mu[m,] <- colMeans(y, na.rm = TRUE)
        Cov[m,,] <- var(y, na.rm = TRUE)
```

```
        vi<- (mu[m,1]/mu[m,2])
        ndvi<- ((mu[m,1]-mu[m,2])/(mu[m,1]+mu[m,2]))
    }

    if((sqrt(Cov[m,1,1])>30)|(sqrt(Cov[m,2,2])>30))
    {
        V$class_id[i] <- 1    #mixed parcel
    }else if((ndvi<0))
    {
        V$class_id[i] <- 2      #uniform bare land
    }else
if(((ndvi>0)&(ndvi<0.1))&((sqrt(Cov[m,1,1])<15)&(sqrt(Cov[m,2,2])<15)))
    {
        V$class_id[i] <- 3       #uniform sparse vegetation
    }else if(((ndvi>0)&(ndvi<0.1)))
    {
        V$class_id[i] <- 4       #non-uniform sparse vegetation
    }else
if(((ndvi>0.1)&(ndvi<0.2))&((sqrt(Cov[m,1,1])<15)&(sqrt(Cov[m,2,2])<15)))
    {
        V$class_id[i] <- 5      #uniform normal vegetation
    }else if(((ndvi>0.1)&(ndvi<0.2)))
    {
        V$class_id[i] <- 6       #non-uniform normal vegetation
    }else if(((ndvi>0.2)&(ndvi<0.4)))
    {
        V$class_id[i] <- 7      #dense vegetation
    }

    polygon(polxy,col=pol_col_arr[V$class_id[i]])

}

V$class_id <- as(V$class_id,"integer")

table(V$class_id)

writeOGR(V, paste(Path_out,"/classified_parcels",sep=""),
paste(im.names[m],"parcels",sep=""), driver="ESRI
Shapefile",overwrite_layer=TRUE)

# The End
```

4. RCODE (Final phase classification)

```
rm(list=ls(all=TRUE))
require(rgdal)
require(rgl)
require(maptools)
require(raster)

StartPath <- getwd()

#Defining the root directory
Root <- "E:/Programming/Emani"

Path_in <- paste(Root, "/Input",sep="")
Path_out <- paste(Root, "/Output",sep="")

dir.create(Path_out,showWarnings=FALSE, recursive=TRUE)
```

```
hist.strecth <- function(x)
{
    n <- dim(x)[2]
    for(k in 1:n)
    {
        data <- x[,k]
        cur.lim <- quantile(data,c(0.025,0.975),na.rm=TRUE)
        data <- pmax(cur.lim[1],pmin(cur.lim[2],data))
        data <- floor(255*(data-cur.lim[1])/(cur.lim[2]-cur.lim[1]))
        data[is.na(data)]<-0
        x[,k] <- data
    }
    return(x)
}

Nim <- 4

Nb <- 4

mu <- array(0,c(Nim,Nb))
Cov <- array(0,c(Nim,Nb,Nb))

#============================================================================
============
# Read images
#============================================================================
============
vector.fn <- "27_march_calibratedparcels"
P1 <- readOGR(paste(Path_out,"/classified_parcels", sep=""),
layer=vector.fn)
n.pol <- length(P1)

vector.fn <- "21_april_new_calibrated_calibratedparcels"
P2 <- readOGR(paste(Path_out,"/classified_parcels", sep=""),
layer=vector.fn)

vector.fn <- "june2_final2_calibratedparcels"
P3 <- readOGR(paste(Path_out,"/classified_parcels", sep=""),
layer=vector.fn)

vector.fn <- "19_july_calibratedparcels"
P4 <- readOGR(paste(Path_out,"/classified_parcels", sep=""),
layer=vector.fn)

# Create new shapefile with crop classification

Crop <- P1
#Crop@data <- data.frame(array(0,n.pol))
#names(Crop@data) <- "crop_type"
Crop@data$crop_type <- rep(0,n.pol)


ind <- which(((P1@data$class_id==1))|
((P2@data$class_id==1))|
((P3@data$class_id==1))|
((P4@data$class_id==1)))

Crop@data$crop_type[ind] <- 1            #mixed parcel
```

```
ind <-
which((Crop@data$crop_type==0)&((P1@data$class_id==3)|(P1@data$class_id==4)
|(P1@data$class_id==5)
|(P1@data$class_id==6)|(P1@data$class_id==7))&          #P1
((P2@data$class_id==7)|(P2@data$class_id==8))&
((P3@data$class_id==2)|(P3@data$class_id==3)|(P3@data$class_id==4)|(P3@data
$class_id==5))&
((P4@data$class_id==4)|(P4@data$class_id==5)|(P4@data$class_id==6)|(P4@data
$class_id==7)))

Crop@data$crop_type[ind] <- 2          #permanent grassland

ind <- which((Crop@data$crop_type==0)
&((P1@data$class_id==2)|(P1@data$class_id==3)|(P1@data$class_id==5)|(P1@dat
a$class_id==6))
&((P2@data$class_id==6)|(P2@data$class_id==7)|(P2@data$class_id==8))
&((P3@data$class_id==3)|(P3@data$class_id==4))
&((P4@data$class_id==3)|(P4@data$class_id==5)|(P4@data$class_id==6)|(P4@dat
a$class_id==7)))

Crop@data$crop_type[ind] <- 3                  #temporary grassland

ind <- which((Crop@data$crop_type==0)
&((P1@data$class_id==2))
&((P2@data$class_id==2)|(P2@data$class_id==5))
&((P3@data$class_id==2)|(P3@data$class_id==4)|(P3@data$class_id==5))
&((P4@data$class_id==6)|(P4@data$class_id==7)|(P4@data$class_id==8)))

Crop@data$crop_type[ind] <- 4                  #winter wheat
table(Crop$crop_type)
ind <- which((Crop@data$crop_type==0)
&((P1@data$class_id==2))
&((P2@data$class_id==2))
&((P3@data$class_id==4)|(P3@data$class_id==5))
&((P4@data$class_id==5)|(P4@data$class_id==7)))

Crop@data$crop_type[ind] <- 5                   #seed potatoes

ind <- which((Crop@data$crop_type==0)
&((P1@data$class_id==2))
&((P2@data$class_id==2))
&((P3@data$class_id==2)|(P3@data$class_id==5))
&((P4@data$class_id==5)|(P4@data$class_id==7)|(P4@data$class_id==8)))

Crop@data$crop_type[ind] <- 6                   #sugar beet

table(Crop$crop_type)


writeOGR(Crop, paste(Path_out,"/classified_crops",sep=""), "crops_revised",
driver="ESRI Shapefile",overwrite_layer=TRUE)

# The End
```